Thermal Barrier as a technique of indirect heating and cooling for residential buildings

M. Krzaczek[1*] and Z. Kowalczuk[2]

[1*]Gdańsk University of Technology

Faculty of Civil and Environmental Engineering

80-233 Gdańsk, Narutowicza 11/12, Poland

Tel.: +48 (58) 348 63 40

Fax.: +48 (58) 347 26 96

marek.krzaczek@wilis.pg.gda.pl

[2]Gdańsk University of Technology

Faculty of Electronics, Telecommunication and Informatics

80-233 Gdańsk, Narutowicza 11/12, Poland

kova@eti.pg.gda.pl

Abstract

The paper presents a concept of an indirect heating and cooling technique of residential buildings driven by solar thermal radiation called Thermal Barrier (TB), which is composed of polypropylene U-pipes located inside of external walls. Fluid flows inside a U-pipes system with a variable mass flow rate and variable supply temperature. This creates a semi-surface parallel to wall surfaces and a spatially averaged temperature almost constant and close to the reference temperature of 17°C all year round. The TB technique is used to stabilize and reduce heat flux normal to the wall surface and to maintain its direction from internal air out to ambient air during the entire year. The main intention of this paper is to investigate the thermal performance and stability of Thermal Barrier. A 3D FE model of a prefabricated external wall component containing a TB U-pipe system with flowing fluid is developed using the FE code of ABAQUS. The FE analysis is supported by a novel SVC control system implemented in FORTRAN to simulate real-working conditions. The advantages of the TB heating/cooling technique are outlined.

Keywords: Thermal Barrier, passive heating and cooling system, gain-scheduling, control system, renewable energy source, solar wall.

1. Introduction

The natural, non-renewable sources of primary energy are strongly limited, and the primary energy consumption in buildings increases. At the same time, the global climate rapidly changes. Thus it is essential to reduce the energy consumption and to utilize renewable energy sources. Buildings consume most energy for heating and cooling. The well known methods of reducing the heat losses in buildings increase the thermal resistance of building components. There are, however, limitations in the further decrease of heat losses in a simple way. Buildings still demand energy for heating and cooling to maintain the thermal comfort in the desired range. The only effective way is to utilize renewable energy. The most attainable and renewable is solar energy. However, there are still two problems to be solved in exploiting this idea. The first one is a large difference between a solar energy supply and the heat demand within each season. The second one is related to the question of how to apply the solar energy for cooling.

One of the most effective approaches to the energy management in buildings is the passive heating and cooling supported by active energy supply systems driven by the solar thermal radiation. Solar-thermal-radiation-driven heating technologies use passive and active solar energy to collect solar thermal radiation and to transform the energy into the usable heat. The passivity is related to the building envelope and structure components design, whereas the activity refers to the use of solar collectors for heating a fluid. A detailed review of passive solar heating and cooling technologies is presented by Chan et al. [1]. The authors conclude that active and passive solar designs have several limitations. Active solar technologies need a development of relatively simple, low-cost, small-capacity, and user-friendly systems. Passive solar designs might not be sufficient to provide the indoor thermal comfort, particularly in regions with extreme climate conditions. The authors also suggest that the research need to be carried out towards improving existing solar technologies and accepting market aspects including system efficiency, architectural aesthetics, and cost effectiveness. The difference between the solar energy supply and the heat demand during passive heating still makes a great problem, which is solved mostly with the use of long-term and short-term heat storage systems. Generally, the concepts are based on a large heat capacitance of building materials, ground, and water, or on the latent heat of PCM materials. Schmidt *et al*. [2] present experiences from central solar heating plants with a seasonal storage in Germany. They

discuss different types of existing seasonal and diurnal heat storage systems. The analyzed short-term heat-storage systems supplying heat to buildings in a district model cover 10-20% of the total yearly heat demand for space heating and domestic hot water, whereas the analyzed long-term heat storage system cover 40-50% of the annual heat demand for domestic hot water. The authors report no major problems during construction. The operational performance of the heat stores is also in an expected range. However, in spite of employing low-temperature heat distribution systems (max. 45°C), the authors report that heating systems have to be supported by heat pumps and electrical heaters which increase the operational temperature.

The recent research results show that there are still problems in applying passive heating/ cooling technologies in practice. Lee *et al*. [3] investigate experimentally an insulation panel which, in addition to the basic functions of common panels, can absorb solar heat. The panel consists of two steel plates with an insulation material and an air layer between them. To stiffen this layer, they employ the insulating material of a honeycomb style instead of a classical one. The air temperature is kept high by the heat gained from a steel plate faced to sun. Depending on the heat demand, the heated air is transferred into the indoor zone or out to the ambient air. The authors [3] indicate that the temperature difference between the entry and exit is about 30K during winter when the wind velocity is about 1 m/s and it is enough for heating. However, the presented concept is useless during summer since it can be used only for heating (and not for cooling). In place of the cooling function, they propose to use the heat gained during summer for domestic hot water. The authors do not consider the possibility of heat storage in a massive layer of external walls to support the heating/cooling function. In contrast, Lee *et al*. [3] and Khalifa *et al*. [4] focus their attention on the ability of external walls to store heat. They study three different materials: concrete and two PCMs. The investigated heat storage systems in external walls are based on the heat of a specific and a latent type. The results confirm that passive heating/cooling technologies can approach the indoor thermal comfort requirements.

Most of passive heating/cooling technologies have some disadvantages. They are close to the thermal comfort, but not enough. Moreover, most of them do not support the cooling function. They need to cooperate with a classical heating/cooling system.

Some recent research results show very advanced active heating and cooling technologies driven by solar energy. Chen Y. *et al.* [5] describe a complex heating system implemented in the two-storey detached low-energy solar house which was constructed in a cold climate area of Canada. The primary heating system is based on a ground heat pump. It is supported by a building-integrated photovoltaic-thermal (BIPV/T) system thermally coupled with a ventilated concrete slab (VCS). An air-based open-loop BIPV/T system produces electricity and collects heat simultaneously. The thermal mass is used both in passive and active forms. The distributed thermal mass in the direct gain area and relatively large south facing triple-glazed windows are employed to gather and store passive solar gains. An active thermal energy storage system stores part of the collected thermal energy from the BIPV/T, reducing the energy consumption of the primary heating system. The house has the annual net energy consumption less than 5000 kWh (about 10% of the national average value) and the annual space heating energy consumption 1600 kWh (i.e. about 5% of the national average value). The integration of a number of the advanced passive and active heating technologies reduces the energy consumption down to almost zero. However, this approach has two great disadvantages: very high construction and maintenance costs.

There are many recent research results which present heating and cooling technologies driven by solar thermal radiation. We recall above only few of those which represent the main stream of investigations. There are, in general, two basic approaches to the energy (non-renewable) consumption reduction:

- passive techniques employing heat storage within external building walls,
- active techniques supplying additional energy to classical heating/cooling systems, with or without heat storing.

Both the approaches utilize solar energy and have many advantages and some disadvantages. This paper presents an idea of Thermal Barrier, constituting a novel approach in the research field to heating and cooling of residential buildings, whose inspiration can be traced back to the workable plan presented in [24]. This concept, avoiding limitations pointed by Chan *et al*. [1], is a representative of the technique of indirect heating and cooling driven by solar energy stored in a geothermal heat storage system of a very low temperature usually smaller or equal than 20°C. The TB technique maintains advantages of passive and active heating and cooling technologies and does not require any appliances to increase the temperature of a heat source. The resulting TB technique (TBT) is implemented in a U-pipes system located inside external

walls to create a semi-surface. Fluid flowing inside pipes carries energy inwards and outwards external walls. Both variable temperature and mass flow rate of the fluid supply contribute to a constant temperature of a semi-surface during the entire year. Unlike other heating and cooling technologies, TB does not assume heating or cooling the indoor air directly. A critical point for TBT is to maintain a constant temperature of the semi-surface during all year round, what evidently requires a very effective control system. The details of our SVC control system are described in [23]. Our concern in this paper is focused on the thermal stability and performance of TBT and the impact of the fluid flow in pipes on the dynamic behavior of the external wall. A 3D FE model of a prefabricated component of external-walls containing a U pipe system with flowing fluid is developed with the aid of the ABAQUS software package. The FE analysis is governed by an SVC control system [23], implemented as a FORTRAN code, which simulates real-working conditions. Thus the main objectives of this study are:

- analysis of the annual temperature stability of the Thermal Barrier semi-surface and
- determination of the annual thermal performance of the prefabricated external-wall component with TB.

2. The concept of Thermal Barrier in external walls

Thermal Barrier is a technique of indirect heating and cooling which supplies energy not into the internal air but into the external walls: to stabilize the heat flux normal to the wall surface, to reduce significantly its magnitude, and to uphold its direction from the inside to ambience. Physically, Thermal Barrier is a system composed of polypropylene U-pipes of 26 mm outer diameter (Fig.1) forming the semi-surface inside external walls. An average temperature of the TB semi-surface is constant during the entire year. The fluid flowing inside U-pipes carries the energy into or from Thermal Barrier. The variable fluid mass flow rate (kg/s) and variable fluid supply temperature maintain a constant average temperature of the semi-surface.

Fig.1

We assume that the operating year temperature of TB is 17°C (± 0.50°C). Thus the heat flux normal to the internal wall surface is almost constant during the entire year and its magnitude is very low. The direction of the heat flux vector goes from the internal air out to ambient air.

It results in maintaining the thermal comfort in a design range, what is equivalent to a heating and cooling function. The heating and cooling system based on the Thermal Barrier technique consists of three main components (Fig.2):

a) the Thermal Barrier U-pipes system inside external walls,

b) low-performance solar panels collecting solar energy,

c) multi-zone geothermal heat storage system.

Fig.2

The TB technique can be supported by any conventional mechanical ventilation system equipped with inlet and outlet elements and a waste heat recovery system. Depending on a particular design, the ventilation system can support TBT to maintain a desired level of the thermal comfort. There can be used any heat storage system or their combination. However, investigating the TB performance and its stability, a simple multi-zone geothermal heat storage system with ground heat exchangers is used. The ground stores energy for TB heating/cooling functions and for warming up the ventilation air. The energy is supplied to a geothermal heat storage system from low-performance solar panels. The structure and design of a geothermal heat storage system is very important for the TB performance, as for each heating/cooling technology. The only difference is that the heating and cooling performance of TB does not strongly depend on the season as compared to other technologies. There are many recent studies on ground heat exchangers for different kinds heating/cooling technologies. Eicker et al. [2] investigate the performance of low depth ground heat exchangers as a heat sink for the building energy produced during summer. They show that ground heat exchangers reach excellent annual coefficients of performance (COP) above 20 using a low pressure drop design. Thus the ground heat exchanger is effective enough to cover the TBT energy demand. However, the TB stability still strongly depends on a heat source temperature and not only on COP of the ground heat exchanger. The temperature and mass flow rate of the fluid supplied to TB U-pipes from a geothermal heat storage system have to be optimally selected and vary in time. It is very difficult to satisfy it by exploiting only one heat source. Hence, instead one variable temperature heat source, several constant temperature heat sources are used. Because the fluid supply temperature depends on a ground temperature and its distribution, a geothermal heat storage system is divided into several zones (heat sources) placed in different regions of the ground surrounding the building. There are recent research results on a temperature distribution in the ground problem. Popiel et al.

[7] investigate experimentally a temperature distribution in the ground outside the building basement for two different locations: car park and lawn. They conclude that the boundary between the shallow zone and deep zone of a constant ground temperature is at the depth of about 10 m and the corresponding constant ground temperature is equal 10.25 °C for the ground under a short grass surface (lawn). A problem of a temperature distribution at the fill layer underneath a slab-on-ground structure of a heated building is investigated by Rantala [7]. The study concerns the typical Finnish slab-on-ground structures and climate conditions typical for Southern Finland. During the survey period, the fill temperature varies between 5-14°C underneath the slab edge and between 9–16°C in the slab centre. The results of investigations [7], [8] show that constant temperatures of heat sources can be reached by locating heat exchangers in different ground zones. The ground surrounding the building can be divided at least into three zones: a low temperature zone located outside the building's outline [7], a medium temperature zone located underneath the basement or slab-on-ground structure and near slab edges [8], and a high temperature zone located underneath the basement or slab-on-ground structure and near the slab center [8]. Hence it is assumed in our study that the heat storage system consists of three ideal heat sources: Low Temperature (LT), Medium Temperature (MT) and High Temperature (HT) heat sources. The LT heat source is located outside the outline of the building basement (slab-on-ground), and MT and HT heat sources are located underneath the basement or slab-on-ground structure of a heated building. It is also assumed that the reference building is a residential detached house located in North-East Poland where climate conditions are close enough to conditions considered in investigations [7] and [8]. It is reasonable to assume that the temperature of the ideal LT heat source is slightly lower for North-East Poland than for South-West Poland and equals 8°C. It is obvious that the temperature of the ground underneath the building basement can be easily increased by supplying the solar thermal energy collected by solar panels. Thus we assume that the heat source temperatures of two heat storage zones located in a geothermal space underneath the building basement (slab-on-ground) (Fig.3) are

- 15°C in the MT zone located near slab edges,
- 20°C in the HT zone located near a slab center.

Fig.3

The MT and HT zones of the geothermal heat storage system are supplied by the TB return fluid and solar thermal energy collected in solar roof panels.

The Thermal Barrier performance depends strongly on the fluid temperature flowing along the U-pipe system. To maintain a nearly constant temperature of the fluid all year round, a novel Scheduling Variable Controller (SVC) is developed based on a control technique called the Fuzzy Mixing Gain-Scheduling (FMGS). A great advantage of the proposed FMGS technique is that the Principal Fuzzy Mixing Equation is used both for scheduling controller gains and fuzzy mixing fluids flowing from geothermal heat sources. Such mixing of flowing fluids can be used to additionally optimize the supply fluid temperature which carries the heat inwards and outwards of a TB U-pipe system. The SVC system consists of the following components:

- Geothermal Heat Storage system,
- Thermal Barrier conditioner including the Fuzzy Mixing Block (FMB) managing the fluid supply temperature,
- Scheduling-Variable Time Lag Block (TLB),
- Fuzzy and Linguistic Block (FLB) and
- FMGS-PI controller.

The annual simulation results (Section 4.4) confirm the great effectiveness of our SVC system. The detailed description of the SVC control system can be found in the paper by Krzaczek and Kowalczuk [22].

3. Model of external-wall prefabricated component with Thermal Barrier

The thermal performance of TB is investigated in external walls of a reference residential detached house located in North-East Poland. This house meets passive house requirements. A total volume of the house is 896 m3. A volume of a heated space is 821 m3 and a heated area is 232.6 m2, while the total area of external walls is 285.4 m2. External walls in the house can differ in structure and materials. They can also differ in static thermal characteristics and a dynamic thermal behavior. Passive heating/cooling systems require external walls to have a large thermal resistance and large heat capacitance. From this point of view, Thermal Barrier is a passive heating/cooling system. It is assumed that external walls of the house are multilayer structures of a large thermal resistance and big heat capacitance. Taking into

account relatively higher complexity of multi-layer external walls with a U-pipes system inside, it is assumed that external walls of the house are prefabricated components. The dimensions of prefabricated components are 1500×1000×400 mm3. The external-wall prefabricated component is composed of the following layers (Fig.4):

- inner insulation,
- light concrete core,
- outer insulation.

Fig.4

The material properties of layers are presented in Tab.1.

Tab.1

The steady-state thermal characteristic of the external-wall prefabricated component is defined by the heat transmittance coefficient *U*. The *U*-value for standard conditions according to the ISO standard [8] is

$$U \ = \ \frac{1}{R_i \ + \ R_c \ + \ R_e} \ = 0{,}131 \ \ \frac{W}{m^2 K},$$
(1)

where:
- the convective thermal resistance on external surface [8] [$m^2 K/W$],
- the convective thermal resistance on internal surface [8] [$m^2 K/W$],
- the thermal resistance of solid layers [K/W].

The *U*-value is very low and typical for passive houses. The U-pipe system of TB is located in a symmetry axis of the core layer of the external-wall prefabricated component. Thermal Barrier is created by 5 U-pipes made of polypropylene with the following dimensions:

- outer diameter is 26 mm,
- inner diameter is 20 mm,
- total length is 3014 mm.

9

The inlet of each U-pipe is connected to a common supply system and the outlet of each U-pipe is connected to a common return system. It is assumed that supply and return systems are perfectly insulated. Water is assumed to be an operating fluid flowing through a U-pipes system. However, in real implementation, water should be mixed with antifreeze which can change water physical parameters. The physical parameters of water and polypropylene are presented in Tab.2.

Tab.2

The performance of Thermal Barrier in the external-wall prefabricated component is investigated numerically. The FE method is also applied to simulate the heat transfer in solid layers and a fluid flowing through a U-pipes system. To decrease a number of finite elements and to reduce computing time of the annual simulation, a geometry of the external-wall prefabricated component is reduced to one U-pipe section only (Fig.5).

Fig.5

In real conditions, the temperature distribution in the component (Fig.5) is asymmetric, since the U-pipe inlet temperature is different than the outlet temperature (they are the same for each U-pipe in the external-wall prefabricated component). A reduction is done by cutting the component with adiabatic surfaces. The reduction procedure defines no heat transfer through the adiabatic surfaces, while in a full scale component, the heat is transferred through these surfaces. The reduction procedure is reasonable because the heat balance of the reduced component in a normal direction to the adiabatic surfaces is equal to zero.

3.1 Heat transfer in solid layers of the external-wall prefabricated component

The external-wall prefabricated component is assumed to be a 3D system (Fig. 6). The heat transfer equation for transient conditions in a Cartesian coordinate system is

$$c_p \rho \frac{\partial T}{\partial t} = \lambda \left(\frac{\partial^2 T}{\partial x^2} + \frac{\partial^2 T}{\partial y^2} + \frac{\partial^2 T}{\partial z^2} \right), \qquad (2)$$

where:

c_p - the specific heat under constant pressure [kJ/kg K],

ρ - the density of the wall layer material [(kg/m^3)],

T - the temperature [°C],

t - the time [s].

Fig.6

The heat transfer equation (Eq.2) is completed with boundary conditions. Assuming that the external wall separates indoor zones at the fixed temperature T_i from ambient conditions, the boundary conditions on the surface S_i and S_e are defined by the Newton's law. A heat exchange rate by convection and radiation on the internal surface S_i is defined by the convective/radiative heat transfer coefficient. Consequently, the boundary conditions on the surface S_i are given as follows

$$\lambda \left. \frac{\partial T(t)}{\partial x} \right|_{S_i} = h_i[T_{Fi}(t) - T_i], \tag{3}$$

where:

λ - the thermal conductivity [W/m K],

h_i - the convective/radiative heat transfer coefficient on the internal surface [W/ m^2 K],

$T_{Fi}(t)$ - the internal surface temperature [°C],

T_i - the internal air temperature [°C].

The heat exchange between the external surface S_e and the outdoor environment is considered by convection and radiation separately. Convection is defined by the convective heat transfer coefficient and radiation is defined by the sol-air temperature. The sol-air temperature T_e is the fictitious temperature of the outdoor air, which, in the absence of radiation exchanges on the outer surface of the roof or wall, would give the same rate of the heat transfer through the wall or roof as the actual combined heat transfer mechanism between sun, the surface of the roof or wall and the outdoor air and the surroundings. Hence, assuming the variable ambient conditions, the boundary conditions on the external surface S_e are

$$\lambda \left. \frac{\partial T}{\partial x} \right|_{S_e} = h_e(t)[T_e(t) - T_{Fe}(t)], \tag{4}$$

where:

$h_e(t)$ - the convective heat transfer coefficient on the external surface [W/m² K],

$T_e(t)$ - the sol-air temperature [°C],

$T_{Fe}(t)$ - the external surface temperature [°C].

The boundary conditions on the adiabatic surfaces S_{a1} and S_{a2} are defined as follows

$$q(t)|_{S_{a1}} = 0 \tag{5}$$

and

$$q(t)|_{S_{a2}} = 0, \tag{6}$$

where $q(t)$ is the heat flux normal to the surface, [W/m²].

3.1.1 Ambient climate conditions

The Thermal Barrier stability depends strongly on ambient climate conditions. In order to reach realistic results, the climate data of Typical Meteorological Year (TMY) for the North-East region of Poland (city of Elblag) are chosen. The climate database [11] contains the averaged hourly data (Fig.7) developed according to the ISO methodology [10].

Fig.7

The investigated external wall is vertical and faced to the South. The sol-air temperature *Te* for vertical surfaces can be defined as follows [12], [13]

$$T_e(t) = T_o + \frac{aI(t)}{h_e(t)}, \tag{7}$$

where:

T_o - the outdoor air temperature [°C],

a - the solar absorptivity of outdoor surface of the wall [-],

$I(t)$ - the incident total solar radiation [W/m^2].

The climate database [11] contains pre-calculated values of incident total solar radiation I for each hour of a day for vertical, facing-south surfaces. The sol-air temperature strongly depends on the solar absorptivity. Kontoleon et al. [14] concludes that solar absorptivity, which affects the exterior forcing function, has a very profound effect on the time lag, decrement factor and temperature variation during the transient heat process. A reflective color (white or light painting) of a wall coating is shown in this paper to be the most profitable control feature benefiting the indoor environment during the summer season. Taking the investigation results [14] into account, the absorptivity coefficient 0.65 equivalent to grey painting is selected to simulate realistic and challenging external conditions for TB. Besides the sol-air temperature, wind driven changes of the convective heat coefficient h_e influence the heat exchange rate on the external wall surface. Thus the convective heat coefficient is defined by empirical formula [15]

$$h_e(t) = \max\left[5, \frac{8.6\,v(t)^{0.6}}{l^{0.4}}\right], \tag{8}$$

where $v(t)$ is the wind speed [m/s] and l is the cubical root of the building volume [m].

A number of FORTRAN subroutines are developed to read the data from the climate database and to compute the sol-air temperature and the convective heat transfer coefficient for each time increment of the simulation using ABAQUS. To smooth out variations of the sol-air temperature and the convective heat transfer coefficient, the time-dependent climate variables are approximated locally by a linear function.

3.2 Heat transfer in the fluid flowing through the TB U-pipe system

An efficient energy utilization exchanged between the fluid flowing through a U-pipe system and solid layers of the wall requires fluid flow to be relatively slowly to increase a heat exchange rate and to decrease an energy consumption of plants forcing flow. It is assumed that the maximum fluid flow velocity u is and the maximum mass flow rate per unit area m is . In this study, water is considered as the operating fluid. The maximum water supply temperature in the component's U-pipe system is . The maximum value of

13

the Reynolds number for the above assumptions can be derived from the following formula [16]

$$\mathrm{Re} = \frac{u\,l}{\nu}. \qquad (9)$$

For the supply water temperature equal to $20\,°\mathrm{C}$ and:

u=0.005 $\left[\frac{\mathrm{m}}{\mathrm{s}}\right]$ - the water flow velocity,

l=0.02 [m]   - the characteristic length scale of the pipe duct (inner pipe diameter),

ν=1.006×10⁻⁶ $\left[\frac{\mathrm{m}^2}{\mathrm{s}}\right]$ - the kinematic viscosity,

the maximum Reynolds number is 99.4. Laminar flow in pipes exists when the Reynolds number is less than transitional value 2300 [16]. In many practical problems of the heat transfer in fluids (for most gases and water as well), it can also be assumed that viscosity equals zero. Thus the fully developed laminar flow of an incompressible fluid in the TB U-pipe system is considered. It is further assumed that mechanical and thermal energy exchanges are independent. In other words, it is assumed that variations of water mechanical properties (density and friction factor) with a temperature variation (and vice versa) can be neglected. This is quite reasonable for very low water flow velocities in a TB U-pipe system. Thus only the energy equation is considered. For incompressible water flow

$$\frac{\partial u_x}{\partial x} + \frac{\partial u_y}{\partial y} + \frac{\partial u_z}{\partial z} = 0. \qquad (10)$$

Neglecting the energy dissipation and assuming that

$$\frac{\partial p}{\partial t} + u_x \frac{\partial p}{\partial x} + u_y \frac{\partial p}{\partial y} + u_z \frac{\partial p}{\partial z} = 0, \qquad (11)$$

what is reasonable for fluid velocities much less than the Mach number, the energy equation can be simplified to the well known form of the Kirchhoff-Fourier [16] energy equation

$$\frac{\partial T}{\partial t} + u_x \frac{\partial T}{\partial x} + u_y \frac{\partial T}{\partial y} + u_z \frac{\partial T}{\partial z} = \frac{\lambda}{\rho c_p} \nabla^2 T. \qquad (12)$$

Hence, the integral formulation of the thermal equilibrium equation within continuum in which a fluid flows with a velocity **u** is as follows [17]

$$\int \delta T \left[\rho c \left(\frac{\partial T}{\partial t} + \mathbf{u} \cdot \frac{\partial T}{\partial \mathbf{x}} \right) - \frac{\partial}{\partial \mathbf{x}} \cdot \left(\mathbf{k} \cdot \frac{\partial T}{\partial \mathbf{x}} \right) - q \right] dV + \int_{S_q} \delta T \left[\mathbf{n} \cdot \boldsymbol{\lambda} \cdot \frac{\partial T}{\partial \mathbf{x}} - q_s \right] dS$$

$$= 0, \tag{13}$$

where:

$T(\mathbf{x}, t)$ - the temperature at a point,

$\delta T(\mathbf{x}, t)$ - the arbitrary variational field,

$\rho(T)$ - the fluid density,

$c(T)$ - the specific heat of fluid,

$\lambda(T)$ - the conductivity of the fluid,

q - the heat added per unit volume from external sources,

q_s - the heat flowing into the volume across the surface on which temperature is not prescribed (S_q),

n   - the outward normal to the surface,

x   - the spatial position,

u   - the vector of velocity,

t - the time.

Eq.13 for the fluid flowing through a TB U-pipe system is completed with equations of boundary conditions. The supply temperature T_r and the fluid flow velocity u can vary in time

$$T_r(\mathbf{x}, t)|_{S_i} = f(\mathbf{x}, t)|_{S_i}, \tag{14}$$

$$\mathbf{n} \cdot \mathbf{u}(t)\,|_{S_i} = u(t), \tag{15}$$

where S_i is the surface of the U-pipe inlet. The fluid velocity u is expressed by the mass flow rate m (kg/s) of the fluid per unit area. The velocity u is computed from the mass flow rate m and the fluid density ρ.

3.3 FE model of external-wall prefabricated component

The FE method is applied to solve the problem of the heat transfer in solid layers of the external-wall prefabricated component and fluid flowing through a TB U-pipe system. To solve a transient heat transfer problem for a 3D system, the ABAQUS software package [17] is applied. The solid layers and the U-pipe system are discretized with diffusive heat transfer 8-node linear brick elements (Fig.8).

Fig.8

In turn, the fluid flowing through a U-pipe system is discretized with convection/diffusion 8-node elements with dispersion control (Fig.9).

Fig.9

Both FE models use interface elements which simulate a convection/diffusion gap between surfaces. The interface elements modify heat exchange conditions in a thin thermal layer of the flowing fluid. The gap clearance is assumed to be 0,2 mm. The Kirchhoff-Fourier equation (Eq.12) assumes a constant fluid velocity profile causing the velocity to be different than zero at the place of the fluid in contact with the U-pipe inner surface. In real laminar flow of an incompressible fluid, there is a thin layer near the pipe surface where the fluid velocity decreases to zero. In this thin layer, heat is transferred mostly by diffusion. The heat transfer between the interface surfaces (fluid-pipe) is defined as follows

$$q = k(T_A - T_B), \tag{16}$$

where:

q	- the heat flux per unit area crossing the interface from point A on one surface to the point B on the other one [W/m^2]
T_A, T_B	- the temperatures of the points on the surfaces [°C],
$k = k(\text{Nu}_{ar})$	- the gap conductance [W/m^{2}K],
Nu_{ar}	- the average magnitude of the Nusselt number [-].

16

The heat transfer condition is related to the Nusselt number. The Nusselt number is determined from the empirical formula introduced by Sieder et al. [18] and is related to the average temperature of interface surfaces and an average fluid mass flow rate

$$Nu_{ar} = f(\bar{T}, |\bar{\bar{m}}|) \tag{17}$$

with

$\bar{T} = \frac{1}{2}(T_A + T_B)$ - the average surface temperature at A and B [°C],

$|\bar{\bar{m}}| = \frac{1}{2}(|\dot{m}|_A + |\dot{m}|_B)$ - the average mass flow rates per unit area of interface surfaces at A

and B [kg/s].

The control method of the gap conductance is coded in the FORTRAN subroutines. The complete FE model is presented in Fig.10.

Fig.10

The maximum time increment is usually the most critical issue for the computation time. The time increment is related to the fluid flow velocity u, which is expressed in terms of the mass flow rate m (kg/s) of the fluid per unit area. The mass flow rate strongly limits the time increment. Due to technical limitations of the TB heating/cooling technique, the mass flow rate m can vary merely from 0.0 to 3.0 kg/s at each time step of the analysis. For convection/diffusion problems, ABAQUS uses a Petrov-Galerkin discretization method [6], which couples a linear temperature interpolation with certain weighting functions. For a numerical stability, the local Courant number C [7] of the convection/diffusion elements should be less than or equal to 1. Due to the complexity of the system geometry and the time-dependency of the velocity vector, initial simulations of a steady-state problem were carried out for different values of the mass flow rate m in order to determine a relationship between the mass fluid flow rate m and maximum time increment Δt. A relationship between m and Δt is demonstrated in Fig.11.

Fig.11

This relationship can be approximated by the exponential function *f(m)*

$$f(m) = 9{,}9298\ m^{-1{,}002}. \tag{18}$$

The time increment control function *f(m)* is implemented in the FORTRAN subroutine to control the current time increment Δt.

4. The numerical results

The main objectives of numerical investigations are to determine:

a) the influence of the mass fluid flow rate on a thermal dynamic behavior (expressed in time lag and decrement factor terms) of the external-wall prefabricated component,

b) the effect of the Thermal Barrier location on a thermal dynamic behavior,

c) the effect of the Thermal Barrier location on the TB semi-surface temperature stability,

d) the annual thermal performance of the external-wall prefabricated component with TB and

e) the annual temperature stability of the TB semi-surface.

The thermal behavior in the cases (a) and (b) is characterized by the time lag φ and the decrement factor (defined in Section 4.1). The TB location impact on the thermal behavior and the TB temperature stability (cases (b) and (c)) are investigated with a modified FE model of the external-wall prefabricated component. Unlike the basic FE model, the modified FE model is composed only of two layers: the external insulating layer and light concrete core layer. The total width of the component remains the same. The SVC system controls the mass flow rate *m* and the supply temperature of the fluid in numerical simulations for cases (c)–(e).

4.1 Time lag and decrement factor

At the cross-section of the outer building wall, there are different temperature profiles during any instant of a 1-day period. These profiles are a function of the inside temperature, outside temperature and materials of wall layers. Since the outside temperature changes periodically during a 1-day period, there exist new temperature profiles at any time instant of the day. During this transient process, a heat wave flows through the wall from the outside to inside and the amplitude of this wave shows the temperature and the wavelength shows the time.

The amplitude of the heat wave on the outer surface of the wall is based on solar radiation and convection between the outer surface of the wall and ambient air. During the propagation of this heat wave through the wall, its amplitude decreases depending on the material and thickness of the wall. When this wave reaches the inner surface, it has an amplitude which is considerably smaller than this at the external surface. Hence, the time lag φ is defined as the time required for a heat wave, with a period P, to propagate through the wall up to the internal surface

$$\varphi_{min} = t_{T_{imax}} - t_{T_{emax}}, \tag{19}$$

where:

$t_{T_{imax}}$ - the time in hours when temperature on the internal surface has its maximum [h],

$t_{T_{emax}}$ - the time in hours when temperature on the external surface has its maximum [h].

The decrement factor *f* is defined as

$$f = \frac{T_{imax} - T_{imin}}{T_{emax} - T_{emin}}, \tag{20}$$

where:

T_{emax} - the maximum temperature on the external surface after stabilizing temperature variations [°C],

T_{imax} - the maximum temperature on the internal surface after stabilizing temperature variations [°C],

T_{emin} - the minimum temperature on the external surface after stabilizing temperature variations [°C],

T_{imin} - the minimum temperature on the internal surface after stabilizing temperature variations [°C].

The sol-air temperature $T_e(t)$ includes the effects of the solar radiation combined with the convective heat exchange between the ambient air and external wall surface. It is assumed that this temperature shows sinusoidal variations during 24-h period. Since the time lag and decrement factor depend on material properties (but not on external climate conditions), the driving function of the external temperature $T_e(t)$ is defined as [19]

$$T_e(t) = \frac{|T_{max} - T_{min}|}{2} \sin\left(\frac{2\pi\, t}{P} - \frac{\pi}{2}\right) + \frac{|T_{max} - T_{min}|}{2} + T_{min}, \tag{21}$$

where:

T_{max} - the maximum external sol-air temperature [°C],

T_{min} - the minimum external sol-air temperature [°C],

P　　- the time period of sine function variations [s],

t　　- the time [s].

The temperatures $T_{min} = -5°C$ and $T_{max} = 5°C$ are selected and the indoor air temperature is assumed to be 0°C. The convective/radiative heat transfer coefficients on the internal and external wall surfaces are defined according to the ISO standard [8]: $h_i = 8.1\ W\ /\ (m^2\ K)$ and $h_e = 23\ W\ /\ (m^2\ K)$, respectively. The time period of sine function variations is 86400 s (24 hours).

4.2 Influence of mass fluid flow rate on thermal behavior of external-wall prefabricated component

The thermal behavior of external walls is mostly defined by the time lag φ and decrement factor f. A number of FE simulations were carried out for the external-wall prefabricated component with a TB U-pipe system using ABAQUS. Even though the time lag and decrement factor characterize the harmonic quasi-steady heat transfer, the model of the transient heat transfer is applied. Thus, the FE simulations under transient conditions are continued until the maximum temperature on the internal wall surface satisfies the following condition

$$T_{imax,n+1} - T_{imax,n} < e, \tag{22}$$

where:

n　　　　- the number of the temperature maximum,

e　　　　- the arbitrary error value [°C],

$T_{imax,n+1}$ - the $n+1$ maximum of the internal temperature [°C],

$T_{imax,n}$ - the *n* maximum of the internal temperature [°C].

Initial steady-state conditions are defined for a mean value of the driving function $T_e(t)$. The time lag and decrement factor are computed for different mass fluid flow rates *m*, where *m* varies between 0.05 kg/s and 3.0 kg/s.

A relationship between the mass fluid flow rate and the time lag is in Fig.12a.

Fig.12

The time lag reaches the maximum value of 10.26 hour for the mass flow rate 0,05 kg/s. This is a satisfactory result for the component with the core layer of 0.15 m width of light concrete. Assan [19] investigated numerically the time lag and decrement factor for different building materials. He presented the time lag equal to 10.31 hour for a concrete block of 0.30 m width. The time lag for the external-wall prefabricated component with TB is equivalent to the time lag for the concrete block with a width of 0.30 m. It results mostly from the high thermal capacitance of water flowing through the TB U-pipe system. However, an increasing mass flow rate decreases the time lag. Thus, it is critical for the TB performance to maintain the mass fluid flow rate in a U-pipes system in a zone of relatively high time lag values. The results of FE simulations show also an evident relationship between the mass fluid flow rate and decrement factor (Fig.12b). The decrement factor reaches the minimum at 0.00044 for the mass flow rate of 3.0 kg/s. This result is equivalent to the decrement factor computed by Assan [18] for the cork board of 0.3 m width. It results from a high thermal resistance of the polystyrene layer of 0.3 m total width. However, a decreasing mass flow rate increases significantly the decrement factor. Low values of the decrement factor are related to relatively high mass flow rates (1.0-3.0) kg/s (Fig.12b). The results show a conflict between optimum values of the time lag and the decrement factor. Thus, the optimum mass fluid flow rate is about 1,0 kg/s. However, when considering technical requirements of the TB supply system, the optimum range of the mass fluid flow rate varies between 0.0 kg/s and 1.0 kg/s, while the operational range varies between 0.0 kg/s and 3.0 kg/s.

4.3 Influence of Thermal Barrier location on temperature stability and dynamic behavior of external-wall prefabricated component

The main task of Thermal Barrier is to stabilize the TB semi-surface at a constant temperature. However, the location of Thermal Barrier can influence its stability and a dynamic thermal behavior of the external wall. To determine the influence of the TB location on the TB stability, the FE model of two-layers of the external-wall prefabricated component (Fig.13) is developed.

Fig.13

The modified external-wall prefabricated component is composed of two layers:

- the external insulating layer made of polystyrene (thickness 0.125 m),
- the core layer made of light concrete (thickness 0.275 m).

The material properties are the same as for the basic external-wall prefabricated component (Tab.1). The total thickness of the wall component remains unchanged. Thus, the total U value of the wall component increases up to 0.231 W/m2 K. Such modification of the component structure is done to enforce the influence of the Thermal Barrier location on the temperature stability and its thermal behavior. The thermal behavior is investigated for a constant mass flow rate m of 0.5 kg/s close to its optimum value for each case of the TB location. The investigations consider 5 locations of the TB U-pipe system in a concrete layer. The Thermal Barrier location is defined by a distance d from the external surface of the concrete layer to the axis of symmetry of a TB U-pipe system. The five locations are chosen: $d=30$ mm, $d=75$ mm, $d=100$ mm, $d=150$ mm and $d=200$ mm. The numerical simulations were carried out for each location (Fig.14).

Fig.14

There is no significant influence of the TB location on the thermal behavior of the component. Taking into account the time lag and decrement factor criterion, a TB U-pipe system can be located in any place inside external walls.

Besides the time lag and the decrement factor influence on the TB stability, and consequently on the TB performance, the heat exchange rate between the fluid and solid layers of the wall affects the TB performance. It is obvious that the temperature of the surface without a U-pipe system and its variations in time depend on the surface location in external walls. If the surface is closer to the internal wall surface, its temperature is higher. Under steady-state conditions equivalent to the SVC control system's working mode I [23], the surface with a temperature of 17°C (the case without a U-pipe system) is located 16.9 mm from the external surface of the concrete layer (Fig.15).

Fig.15

Hence the concrete core layer can be divided into two zones: TB Ineffective Zone and TB Effective Zone. As it is shown in Fig.15, the temperature of the surface is close to the reference temperature of 17 °C in TB Ineffective Zone. Thus it is not advisable to place TB in this zone, because a heat exchange rate is close to zero. The TB temperature stability is further investigated only for the most effective location d=30 mm in TB Effective Zone and for the most demanding time period on 15th of February. The SVC control system is re-tuned for a modified model of the external-wall prefabricated component. The results show that SVC maintains the TB temperature very close to its reference value of 17°C (Fig.16).

Fig.16

The TB temperature varies from 16.937°C up to 17.282°C, while the sol-air temperature varies from -12.50°C up to 119.95°C. A mean value of the TB semi-surface temperature is 17.048 °C.

The investigation case is very demanding for the SVC control system. An equivalent value of the decrement factor measured for the TB location is very high. Thus the influence of the sol-air temperature on the TB temperature stability is very pronounced. Nevertheless, the SVC control system still maintains the TB temperature at 17°C. The maximum variation of the TB semi-surface temperature is also in a design range. The TB stability depends strongly on a size of TB Ineffective Zone. The increasing size of Ineffective Zone decreases radically the TB stability. However, TB Ineffective Zone can be eliminated by adding a third layer with a low value of the thermal conductance coefficient, e.g. a layer of AAC. The third layer decreases significantly temperatures in the core layer and increases the TB stability. Thermal

Barrier is not sensitive to its location inside the particular layer but is sensitive to the wall structure and material properties. The optimum design includes a multi-layer structure composed of three layers: the external insulating layer, the massive core layer with a TB U-pipe system and the internal layer of a low-thermal-conductivity material (e.g. AAC).

4.4 Annual TBT performance and TB stability

The specific mechanism of the TB heating and cooling makes the TB performance presentation difficult. TB does not only heat up indirectly the indoor zone but it also cools down. Thus, the TB performance is presented by a comparison with the external-wall prefabricated component without a TB U-pipe system. The TB performance definition is based on the heat flux vector (normal to the internal wall surface). In the case of the external-wall prefabricated component with a TB U-pipe system, the direction of the vector does not change during a year. Unlike the case of a TB U-pipe system inside, if a TB U-pipe system is absent, the vector changes its direction depending on a season (Fig.17).

Fig.17

The direction changes of the vector (Fig.17) correspond to heating and cooling demands of indoor zones. Both, heating and cooling demands require to supply energy to maintain the thermal comfort. We assume that only the heat transferred through the external-wall prefabricated component affects heating and cooling demands of indoor zones. Such assumption lets us express heating and cooling demands as a function of the heat flux on the internal wall surface. Thus the TB performance is defined as a ratio of the annual heating/cooling demand for the external wall without TB and the annual heating demand for the external wall with a TB U-pipe system inside. Hence, the TB coefficient of performance η is defined as

$$\eta = \frac{Q_{Hi} + Q_{Ci}}{Q_{TBi}}, \tag{23}$$

where:

$$Q_{TBi} = -A_{cmp} \left(\int_0^{t_H} \dot{Q}_i(t) \, dt + \int_{t_C}^{t_{max}} \dot{Q}_i(t) \, dt \right), \tag{24}$$

$$Q_{Hi} = -A_{cmp} \left(\int_0^{t_H} \dot{Q}_i(t)\, dt + \int_{t_C}^{t_{max}} \dot{Q}_i(t)\, dt \right), \tag{25}$$

$$Q_{Ci} = A_{cmp} \int_{t_H}^{t_c} \dot{Q}_i(t)\, dt, \tag{26}$$

and

$$\dot{Q}_i(t) = \int_{S_i} \mathbf{n}\, \mathbf{q}_i(t)\, dS \tag{27}$$

with:

Q_{TBi} - the energy transferred from the indoor zones out to the ambient air during one year time period (case with TB U-pipe system) [kJ],

Q_{Hi} - the energy transferred from the indoor zones out to the ambient air during heating periods (case without TB U-pipe system) [kJ],

Q_{Ci} - the energy transferred from the ambient air to the indoor zones during cooling period, (case without TB U-pipe system) [kJ],

$\dot{Q}_i$ - the energy transferred through the surface per time unit [kW],

t_H - the time of first period of heating demand [s],

t_c - the time of period of cooling demand [s],

t_{max} - one year time period [s],

S_i - the internal surface of the external-wall prefabricated component [m^2].

It can also be expressed as the ratio of the energy amount transferred through the external-wall prefabricated component with a TB U-pipe system from the indoor zone out to the ambient air during heating periods, and as the energy amount transferred through the external-wall prefabricated component without a TB U-pipe system during heating and cooling periods. The heating and cooling periods are determined according to annual variations of the heat flux $q_i(t)$ on the internal wall surface without a TB U-pipe system (Fig.17).

The TB stability is defined as the maximum TB temperature error $e_{max} = \max\limits_{t}(|e(t)|)$, where $e(t) = T_b(t) - T_{bref}$. The annual TBT performance and TB stability are investigated

numerically with a FE model (Fig.10) of the external-wall prefabricated component with and without a TB U-pipe system [17].

The numerical simulations are performed using the ABAQUS software package. Several existing user subroutines were modified and several new subroutines were implemented (Fig.18) for:

- climate data processing to compute the sol-air temperature and convective heat transfer coefficient,
- data processing of temporary results in each step and time increment of our FE analysis,
- managing the entire FEA process,
- updating boundary conditions of heat transfer in solid layers and in the fluid in each step and time increment of FEA,
- improving a heat exchange between the flowing fluid and U-pipe solid body,
- generating final results of FEA in each time increment.

Fig.18

The SVC controls the mass fluid flow rate m and fluid supply temperature T_s. The SVC updates boundary conditions of the heat transfer in the fluid flowing through a TB U-pipe system. The ambient climate conditions are defined by data in North-East Poland [11]. The annual numerical simulations are performed for two cases:

a) the external-wall prefabricated component with a TB U-pipe system and
b) the external-wall prefabricated component without a TB U-pipe system.

The results of FE annual simulations for the case 'a' show that the TB temperature stability is preserved during the entire year. The TB stability is significantly smaller than the design value of 0.5 °C. The TB temperature is almost fixed at 17°C (Fig.19) and the mean value of the temperature is exactly 16.997°C varying solely within a small range of -0.147 - 0.216°C.

Fig.19

The SVC control system maintains not only the TB semi-surface temperature very close to the reference value but also optimizes the fluid supply temperature (Fig.20) by mixing fluids [23].

Fig.20

Due to the almost constant TB semi-surface temperature, the heat flux on the internal surface of the external wall varies slightly within a small range of -1.104 - -0,651 W/m^2 (Fig.21).

Fig.21

Assuming that the TB semi-surface temperature is constant and equal to the reference temperature of 17°C, the heat transfer conditions in layers between the TB semi-surface and the internal wall surface are equivalent to steady-state conditions. The magnitude of the heat flux under steady-state heat transfer conditions is s (Fig.21). As it is shown in Fig.21, the heat flux varies slightly around the steady-state heat flux of . The median value of the heat flux is and is similar as the steady-state heat flux. Thus, Thermal Barrier stabilizes the heat flux on the internal wall surface and enforces the indoor zone heating/cooling process. The heat exchange rate between the fluid flowing through a TB U-pipe system and solid layers of the wall is characterized by the total amount of energy transferred from/to the fluid. Depending on ambient conditions, the fluid supplies energy into the wall or extracts energy from the wall. Fig.22 presents the cumulated diagram of the total amount of energy transferred from/to the fluid during one year time period.

Fig.22

The energy is supplied to the external wall during 151 days and is extracted from the external wall during 214 days. More energy is extracted from the external-wall prefabricated component during one year time period than it is supplied. The total annual energy amount extracted from a geothermal heat storage system is 15.82 MJ, while the total annual energy amount returned to a geothermal heat storage system is 27.81 MJ. Thus, the annual energy balance in a geothermal heat storage system is positive. The results (Fig.22) show that a geothermal heat storage system stores the energy of 12.01 MJ, i.e. more than it releases during one year. Thus, Thermal Barrier is the self-sufficient heating/cooling system. However, the numerical investigations are carried out only for the external wall faced to South. The external walls faced to other geographical directions (particularly to North) collect the smaller energy

27

during the same time. Moreover, the energy is carried from a TB U-pipe system by the fluid with a mean value of the return temperature equal to 16.87°C and varying within a range of 15.64 – 17.79 °C (Fig.23).

Fig.23

The relatively low return temperature of the fluid results in a heat exchange rate decrease in the ground heat exchanger. Thus, the fluid returning from a TB U-pipe system can be returned only to the MT zone (15°C) of a geothermal heat storage system, while the HT zone (20 °C) is to be still supplied with the heat from solar thermal roof collectors. The above results are not surprising. The passive solar walls are used to collect and store solar energy which can contribute to the building heating. Different approaches exist to a solar walls design in the recent research [20]. Both, classic and composite solar walls usually store the solar thermal energy to warming up the ventilation air. Unlike solar walls, the TB technique utilizes the solar energy primarily to support the SVC control system in stabilizing the TB semi-surface temperature and secondarily to supply heat to the MT zone. The energy required to cover annual heating and cooling demands in the case of the component without a TB U-pipe system is much higher than the energy required to cover the annual heat demand in the case of the component with a TB U-pipe system (Fig.24).

Fig.24

The annual TB coefficient of the performance is . It can be interpreted such that Thermal Barrier reduces heating and cooling demands at least three times as compared to the traditional external wall without Thermal Barrier. However, we have to note that our numerical investigations were performed only for the external wall faced to South. Moreover, we met several assumptions limiting the more general conclusions. Nevertheless, following the above assumptions and focusing an analysis of TBT advantages on a decrease of heat losses through external walls only, the influence of the TB technique on the total annual heat demand of the reference residential house can be estimated. The annual heat losses through external walls of the reference residential house, calculated according to the ISO standard [21], are 3283.2 kWh/a, while the total heat losses are equal to 9801.5 kWh/a (Tab.3).

Tab.3

The total annual heat demand for the reference residential house is 2245.4 kWh/a. The heat losses through external walls with prefabricated components including TB are 1118.6 kWh/a, while in the case of the external wall without TB are 3283.2 kWh/a. The TB technique decreases the heat losses through external walls by 2164.6 kWh/a, and it is very close to the total annual heat demand.

According to our FE simulations, an increase of the fluid reference temperature up to 20°C (instead of 17°C) further improves the TB performance. The SVC control system is able to change the fluid reference temperature in the range of 17ºC–20ºC, while the control settings can be modified by residents to meet the indoor thermal comfort. The maximum reference temperature of the fluid flowing in the U-pipe system strongly depends on the heat exchange rate in the ground storage system. In order to increase the Thermal Barrier performance and to develop necessary design procedures, the investigations have to be continued on the real model of the residential building coupled with the ground heat storage system.

5. Conclusions

Unlike passive solar walls and passive heating/cooling systems, Thermal Barrier utilizes the solar energy to support the SVC control system [23] in stabilizing the TB semi-surface temperature and supplying the energy to the cooperative geothermal heat storage system. The results of annual FE simulations confirm an excellent performance and effectiveness of the approach. The TB temperature is fixed at 17°C varying solely within a small range of -0.147-0.216°C during the entire year.

The FE simulations have shown that the maximum time lag is 10.26 h and the minimum decrement factor is 0.00044. The optimum range of the mass fluid flow rate is 0.05-1.0 kg/s. No significant influence of the TB location on the thermal behavior of the external-wall prefabricated component has been found. However, when considering the TB performance, it is not advisable to locate TB in the Ineffective Zone of the external wall which can be eliminated by adding a third layer with a low value of the thermal conductance coefficient. The TB stability is not sensitive to the location in a particular layer but to the wall structure (e.g. the number of layers) and the material properties of layers. Thus the optimum design of the external wall with TB is a multi-layer structure composed of at least three layers: the

external insulating layer, the massive core layer with a TB U-pipe system and the internal layer of a low-thermal-conductivity material.

TB reduces heating and cooling demands at least three times as compared to the traditional external wall without TB. More energy is extracted from the external wall with TB than is supplied during one year. However, the energy is returned from the TB U-pipe system by the fluid with the mean value of the return temperature of 16.87°C. Thus the fluid returning from the TB U-pipe system can be supplied only to the MT zone (15 °C) of the geothermal heat storage system.

A TB implementation in residential houses meeting the passive house requirements is capable of decreasing the total annual heat demand (heating and ventilation only) almost to zero. Considering, however, both the heating and the cooling process, the TB advantages become more pronounced. The TB temperature almost fixed at 17°C radically reduces the risk of a water vapor condensation inside the layers bounded by the TB semi-surface and the internal wall surface, as well as on the internal wall surface. It enables us to design insulating layers by the indoor side of external walls. The TB technique can thus be implemented successfully both in new building designs or in thermo-modernizations of existing buildings.

Our research will be continued. In the next stage, a model house will be built to check the performance of the Thermal Barrier and its ability to maintain the designed thermal comfort conditions.

Acknowledgements

References

1. Chan, H. Y., Riffat, S. B. and Zhu, J. Review of passive solar heating and cooling technologies. *Renewable and Sustainable Energy Reviews*, 2010, 14:781-789.
2. Schmidt, T., Mangold, D. and Müller-Steinhagen, H. Central solar heating plants with seasonal storage in Germany. *Solar Energy*, 2004, 76:165-174.

3. Lee, S., Kim, S., Kim, S., Park, Y. and Park, J. Experimental research on performance of the solar heat gain (SHG) insulation panel. *Building and Environment*, 2006, 41:336-342.

4. Khalifa, A. and Abbas, E. A comparative performance study of some thermal storage materials used for solar space heating. *Energy and Buildings*, 2009, 41:407-415.

5. Chen Y., Athienitis A.K., Galal K., Modeling, design and thermal performance of a BIPV/T system thermally coupled with a ventilated concrete slab in a low energy solar house: Part 1, BIPV/T system and house energy concept. *Solar Energy*, 2010, 84:1892-1907.

6. Yu, C.C. and Heinrich, J. C. Petrov-Galerkin method for multidimensional, time dependent, convective-diffusive equations. *International Journal for Numerical Methods in Engineering*, 1987, 24:2201-2215.

7. Popiel, C. O., Wojtkowiak, J. and Biernacka, B. Measurements of temperature distribution in ground. *Experimental Thermal and Fluid Science*, 2001, 25:301-309.

7. Rantala, J. A new method to estimate the periodic temperature distribution underneath a slab-on-ground structure. *Building and Environment*, 2005, 40:832-840.

8. PN-EN ISO 6946:2008, Building components and building elements. Thermal resistance and thermal transmittance. Calculation method. 2008, (in polish).

9. PN-EN ISO 15927-4, Hygrothermal performance of buildings – Calculation and presentation of climatic data – Part 4. Data for assessing the annual energy for cooling and heating systems. Warsaw, 2007, (in polish).

10. *The climate database of typical meteorological year*. Polish Ministry of Infrastructure. Warsaw, 2009.

11. Threlkeld, J. L. *Thermal Environmental Engineering*. Englewood Cliffs, NJ: Prentice-Hall; 1970.

12. Duffie, J. A. and Beckman, W. A. *Solar Engineering of Thermal Processes*. New York: John Wiley and Sons; 1991.

13. Kontoleon, K. J. and Bikas, D. K. The effect of south wall's outdoor absorption coefficient on time lag, decrement factor and temperature variations. *Energy and Buildings*, 2007; 39:1011-1018.

14. Duffie, J. and Beckman, W. *Solar engineering of thermal processes*. New York: Wiley; 1980.

15. Staniszewski B. *Heat exchange. Theoretical fundamentals*. Warszawa: PWN, 1980 (in polish).

16. Dassault Systèmes Simulia Corp., ABAQUS Version 6.8 Documentation. Providence, RI, USA, 2008.

17. Sieder, E. N. and Tate, G. E., Heat transfer and pressure drop of liquids in tubes. *Ind. Eng. Chem.*, 1936, 28:1429-1435.

18. Asan, H. Numerical computation of time lags and decrement factors for different building materials. *Building and Environment*, 2006, 41(5):615-620.

19. Shen, J., Lassue, S., Zalewski, L. and Huang, D. Numerical study on thermal behaviour of classical or composite Trombe solar walls, *Energy and Buildings*, 2007, 39:962-974.

20. ISO 13790, Energy performance of buildings - Calculation of energy use for space heating and cooling, 2008.

21. Eicker, U. and Vorschulze, Ch. Potential of geothermal heat exchangers for office buildings climatisation. *Renewable Energy*, 2009, 34:1126-1133.

22. Krzaczek, M. and Kowalczuk, Z. An effective control system for heating and cooling in residential buildings using Thermal Barrier. *Building and Environment*, 2010 (under review).

23. T.H. Technology Consulting Holding AG, Energy concept of the ISOMAX climate control. Sarnen, Switzerland, 2008.

Figures
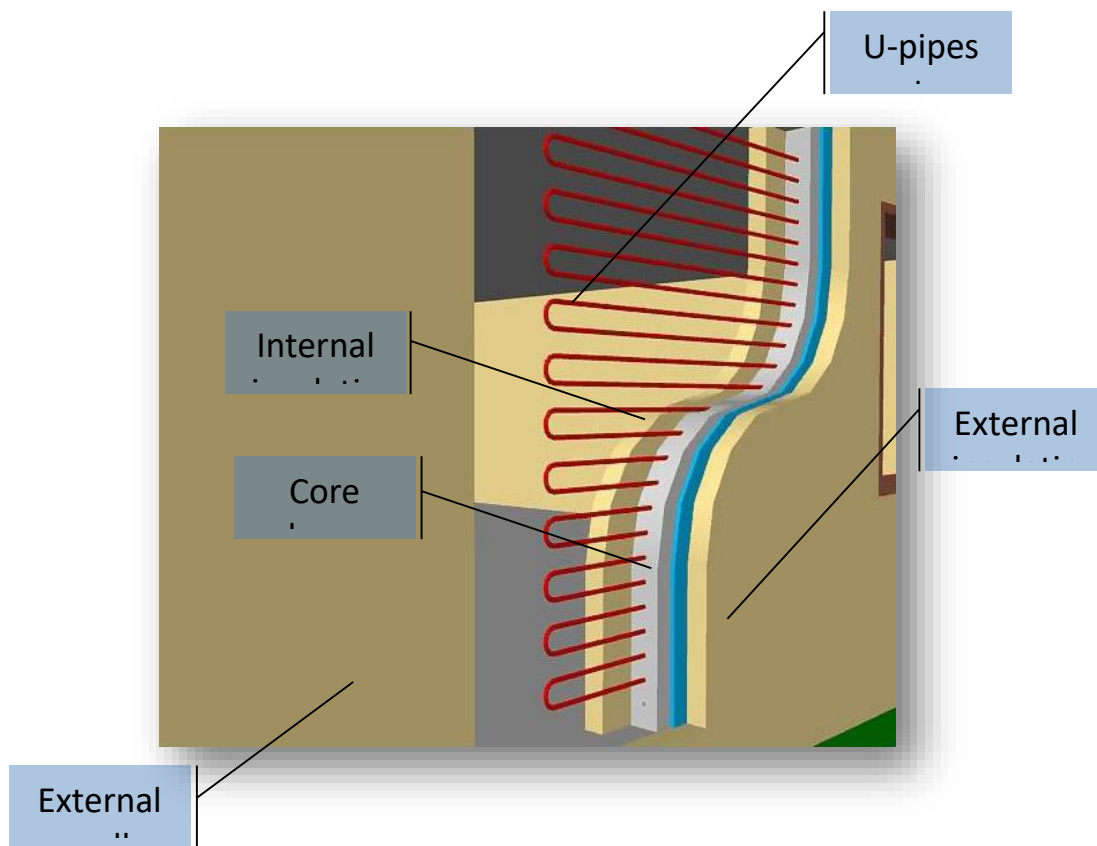
Fig.1: The U-pipes system creating Thermal Barrier inside external walls

Thermal Barrier

Low-performance solar collector

Ground heat exchanger of the geothermal heat storage system
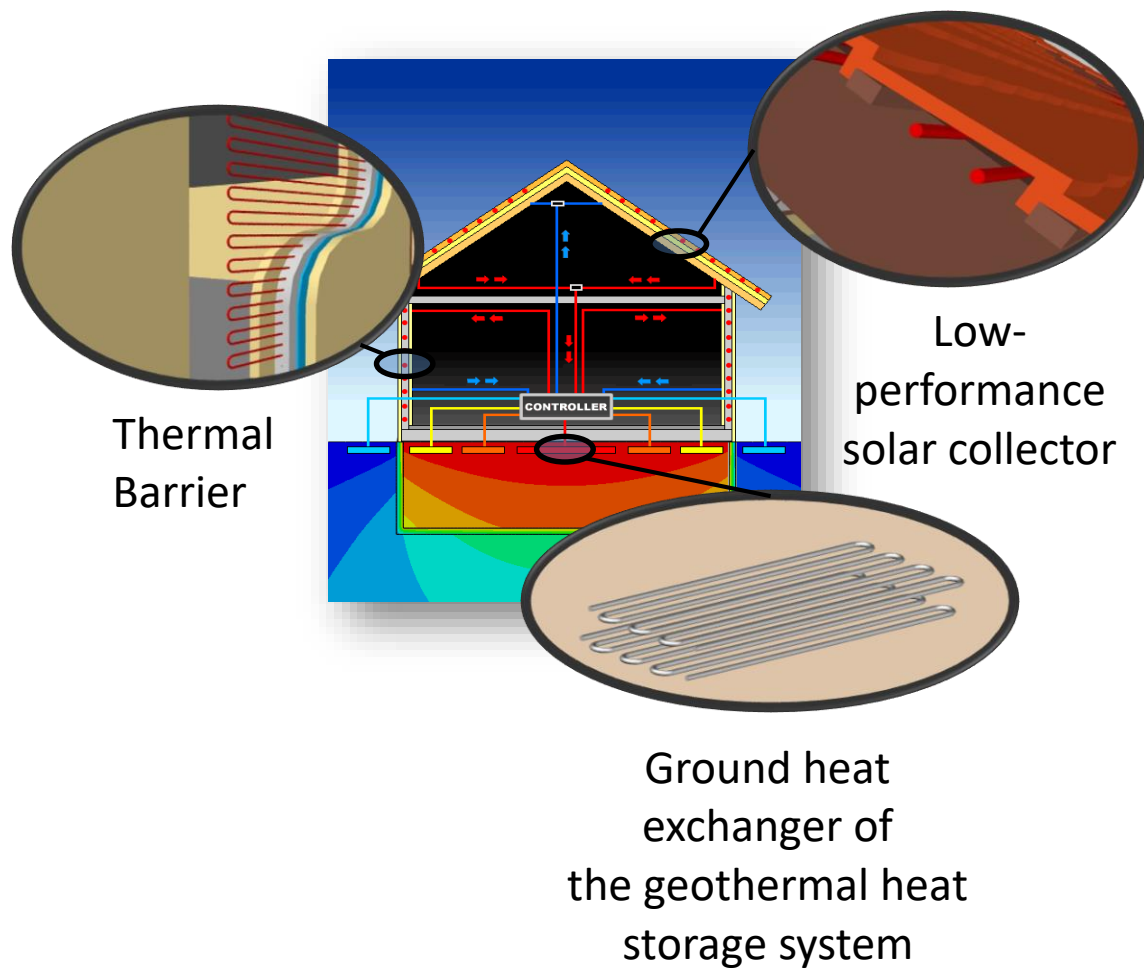
Fig.2: Main components of heating/cooling system based on Thermal Barrier technology
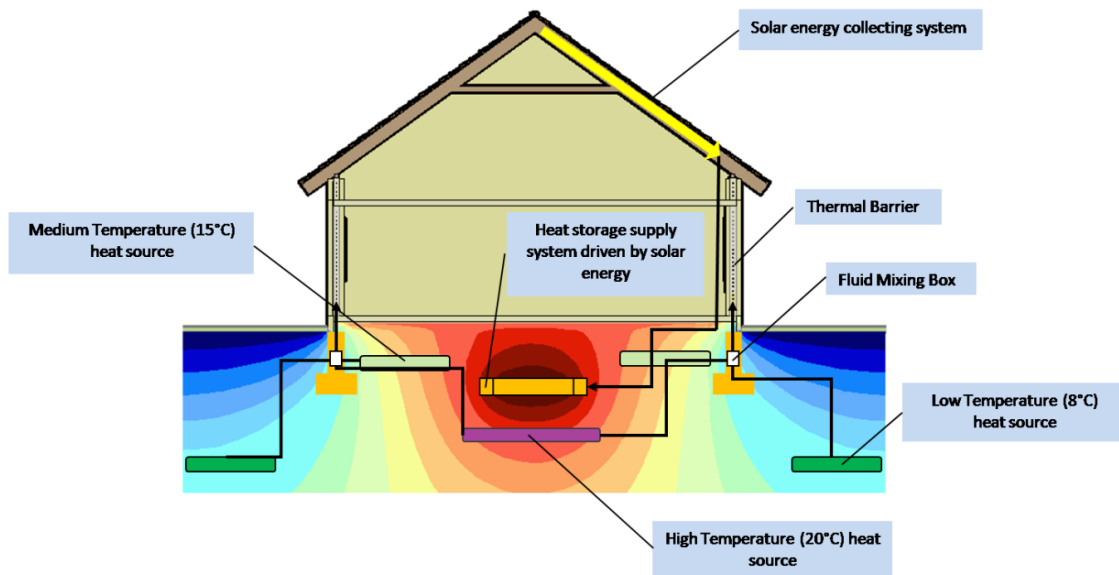
Fig.3: Location of geothermal heat storage zones (heat sources)
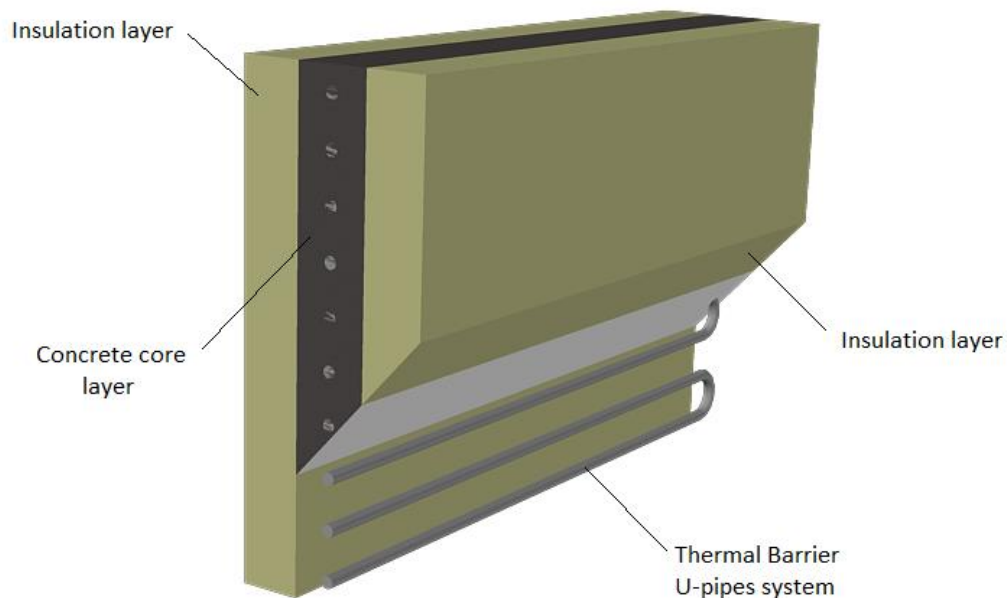
Fig.4: Thermal Barrier: U-pipes system in the prefabricated component of the external wall
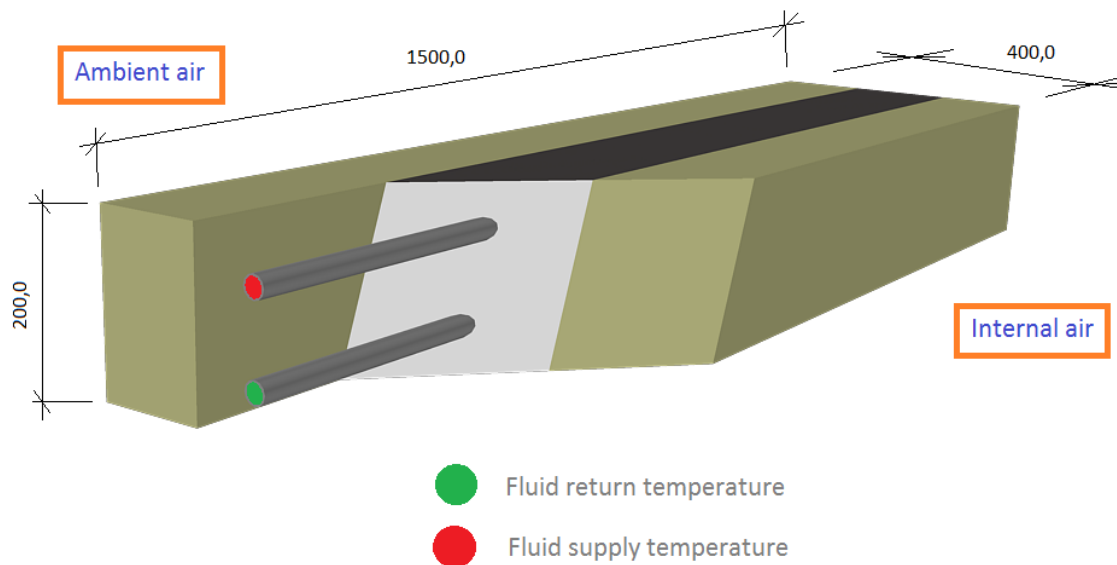
Fig.5: The model of the external-wall prefabricated component
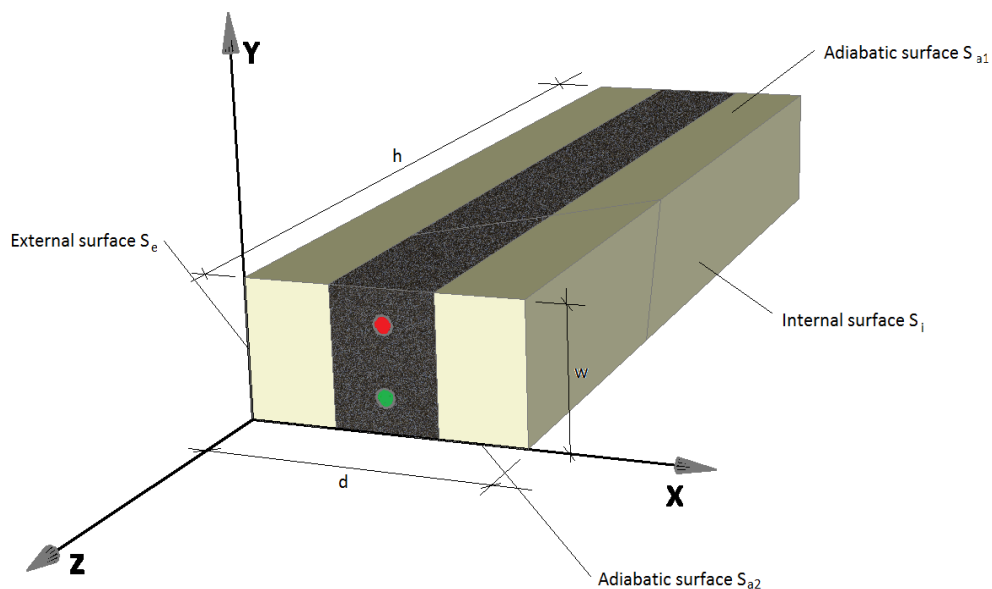
Fig.6: Orientation of the external-wall prefabricated component with TB in Cartesian coordinate system

a)
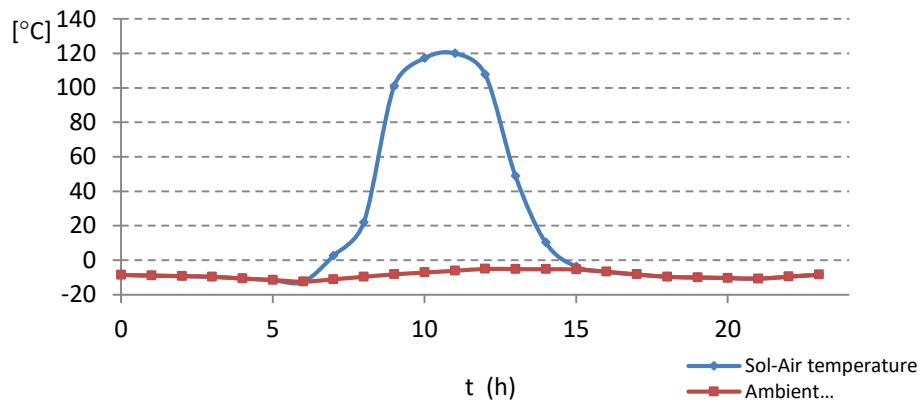
b)
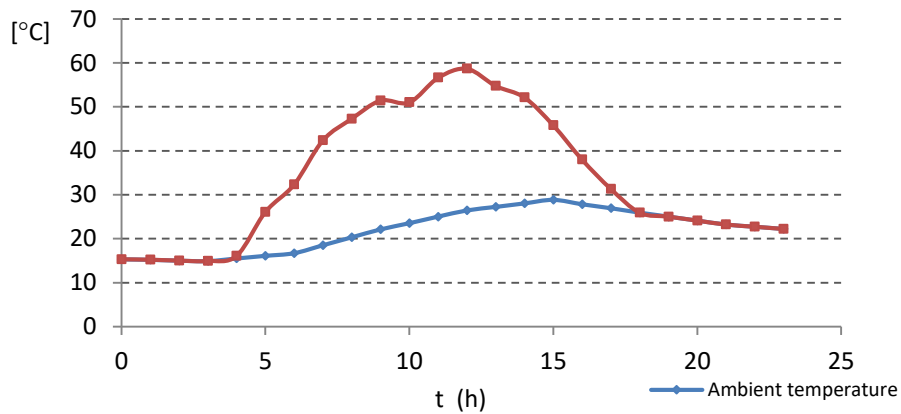
c)
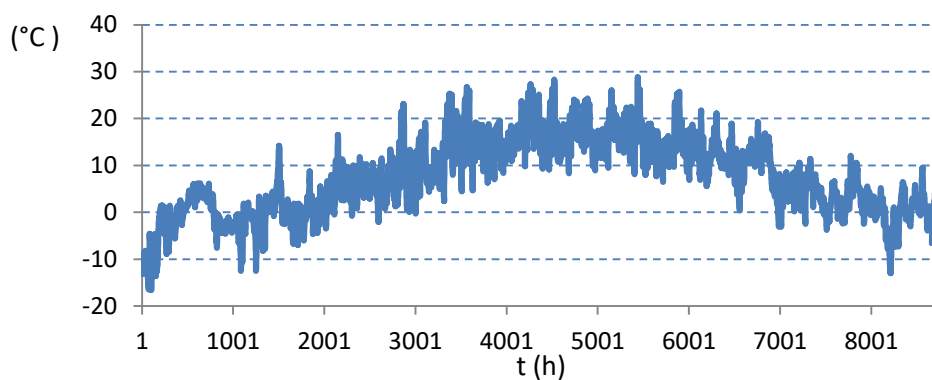
Fig.7: Climate data of Typical Meteorological Year: a) a day of the highest sol-air
temperature (February 24th), b) the hottest day for ambient temperature (August 15th),
c) hourly averaged ambient air temperature (one year time period)
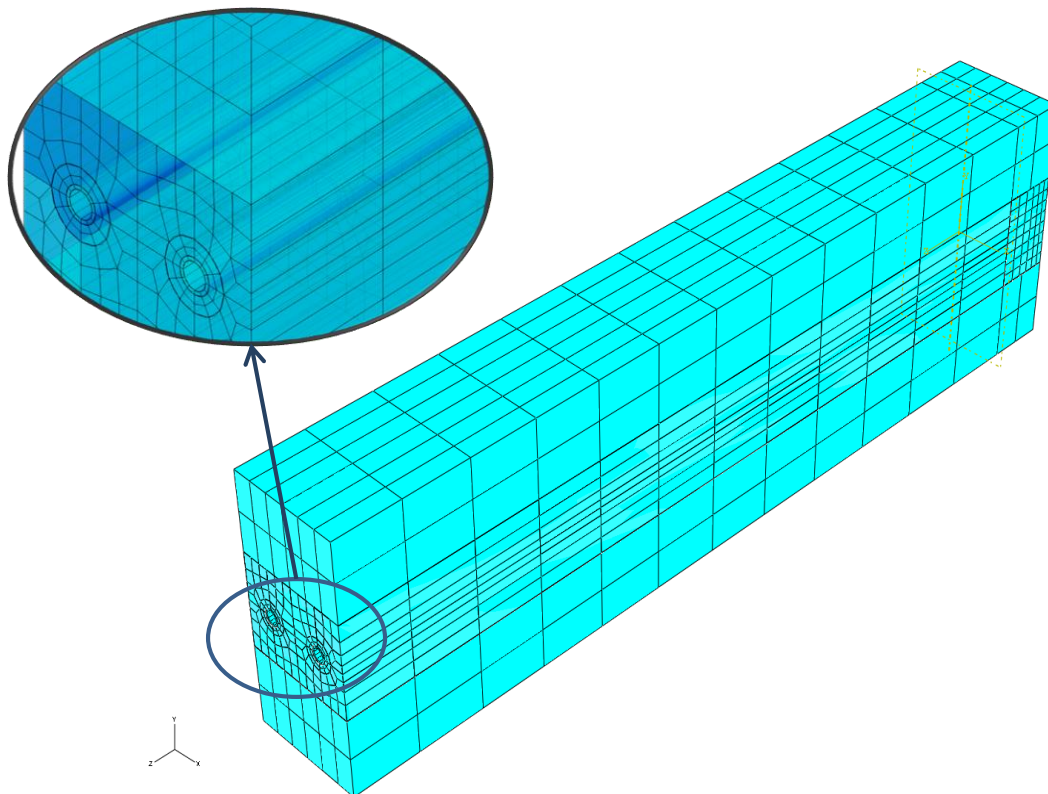
Fig.8: FE model of solid layers and U-pipe system discretized with diffusive heat transfer 8-node linear brick elements
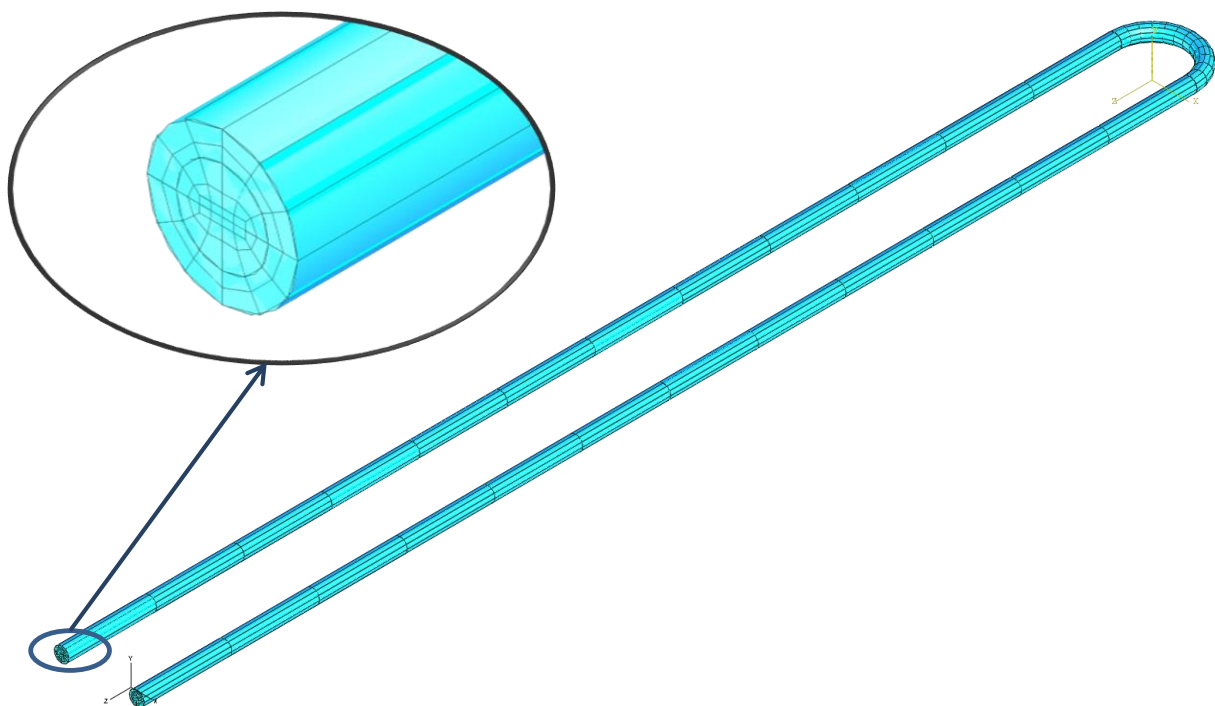
Fig.9: FE model of flowing fluid discretized with convection/diffusion 8-node elements with dispersion control.
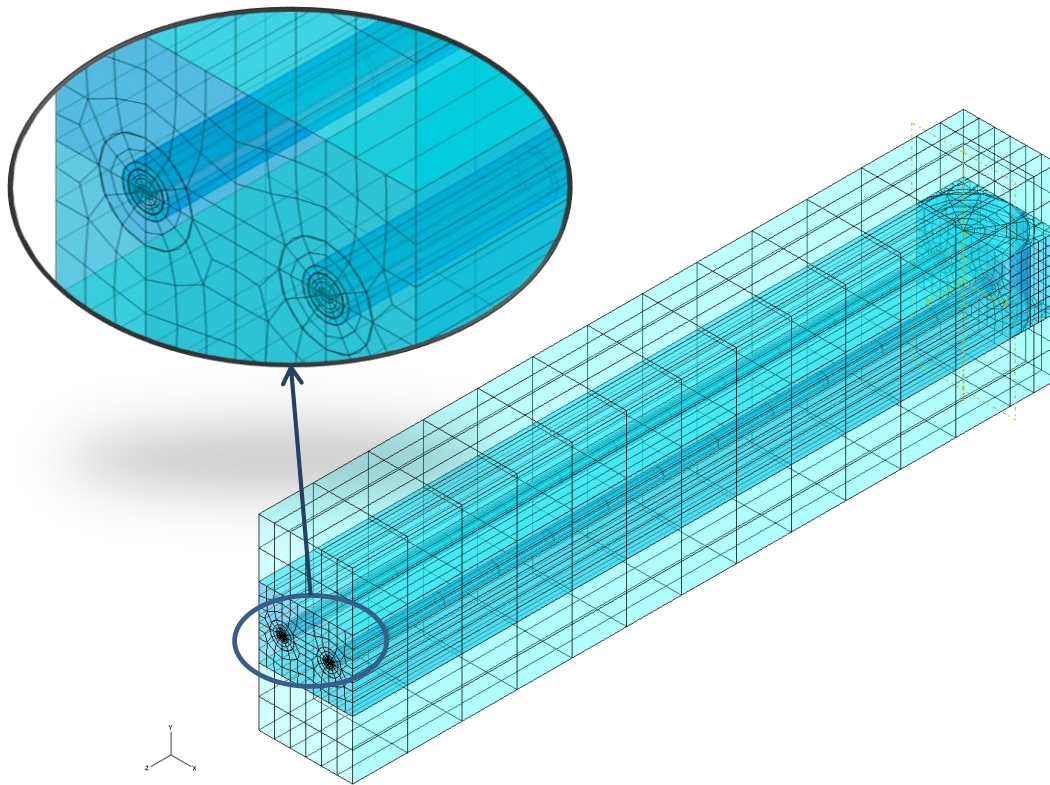
Fig.10: The complete FE model of the external-wall prefabricated component with Thermal Barrier (using U-pipe system)
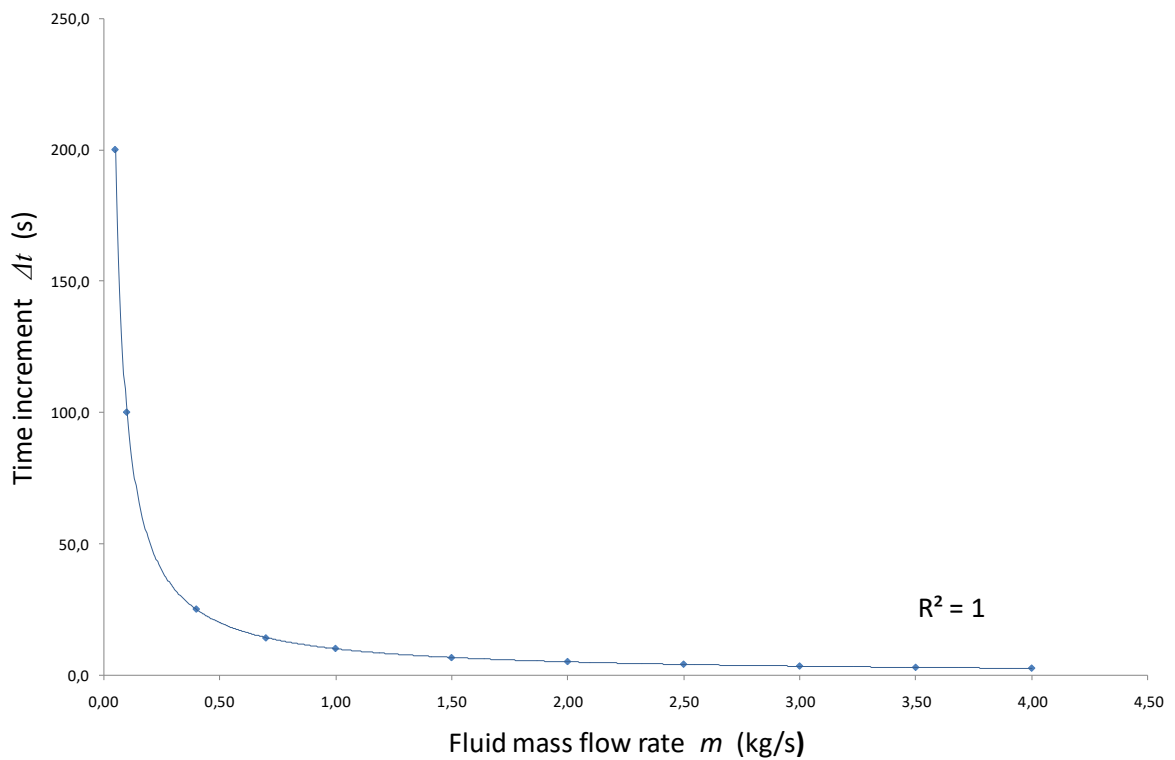
Fig.11: The relationship between mass fluid flow rate *m* and maximum time increment Δt

(a)
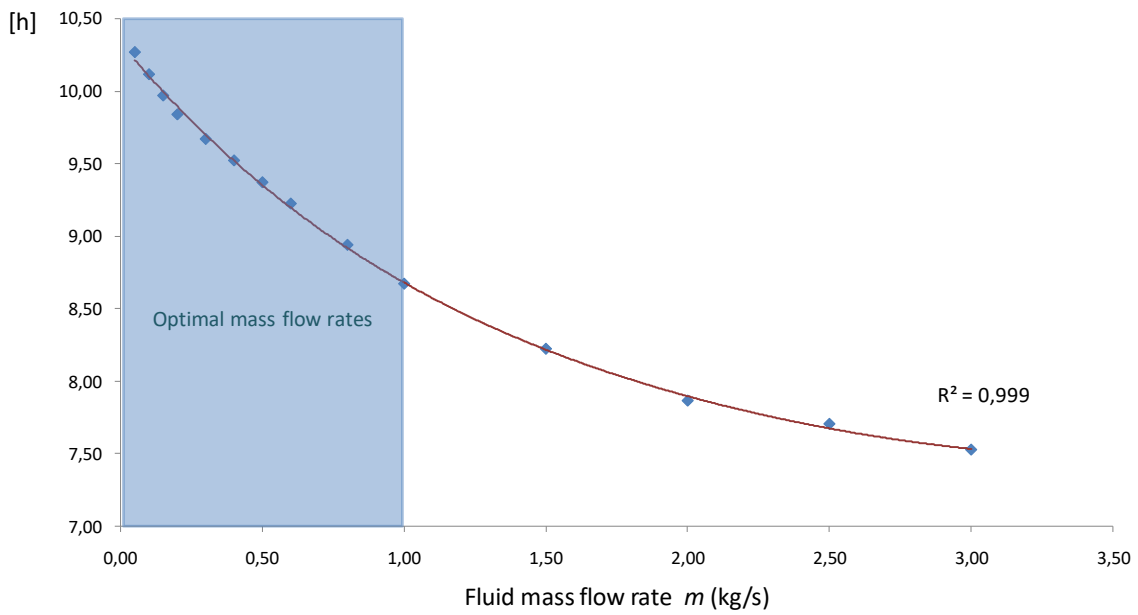
(b)
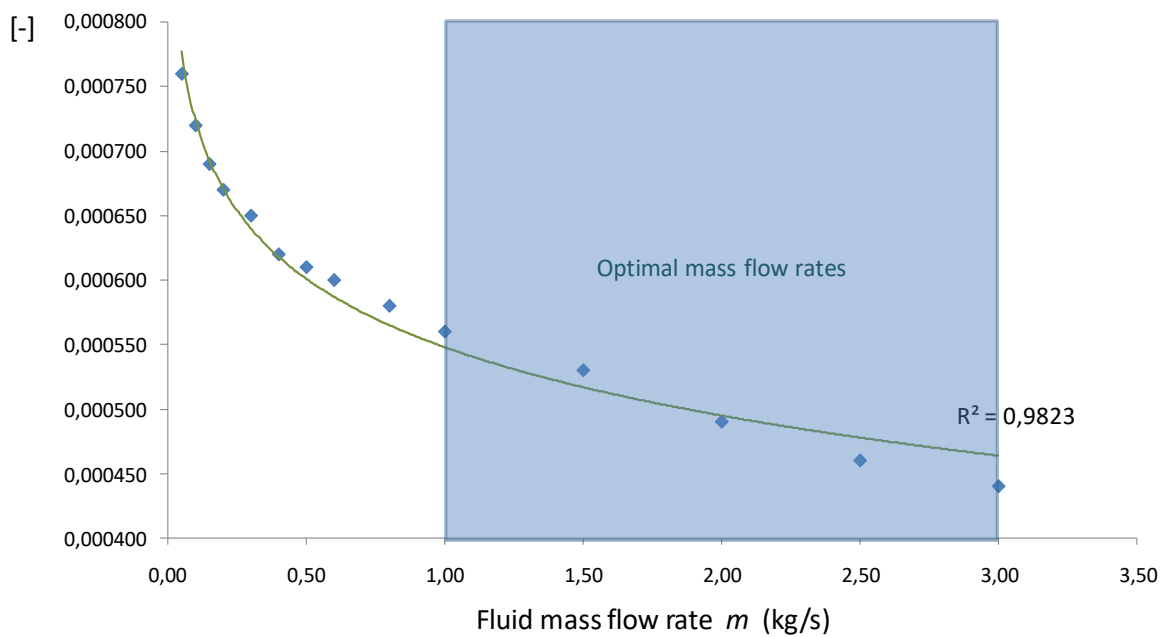
Fig.12: The fluid mass flow rate m versus: the time lag (a) and the decrement factor (b) (m varies between 0.05 kg/s and 3.0 kg/s)
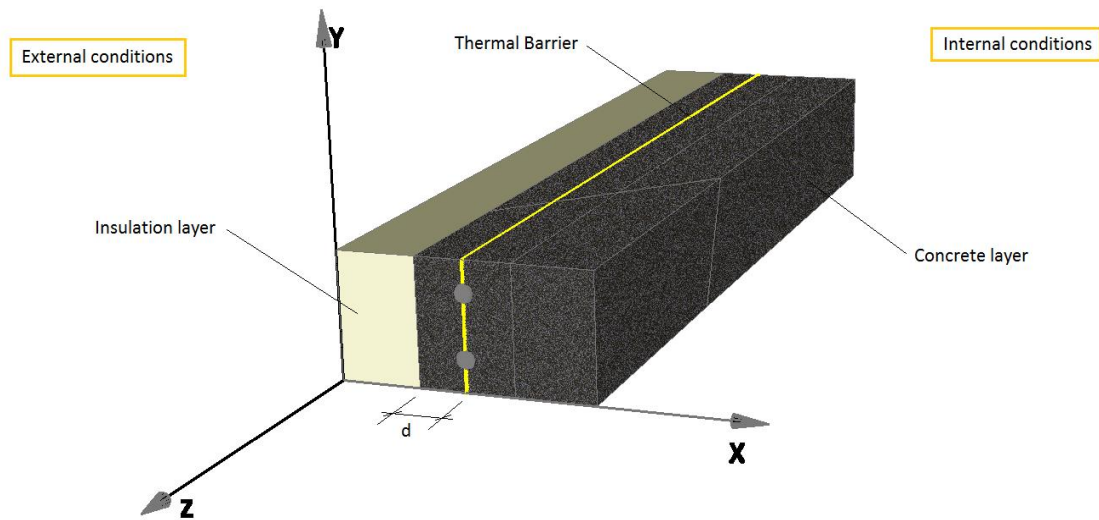
Fig.13: The modified model of the external wall component with the variable TB location
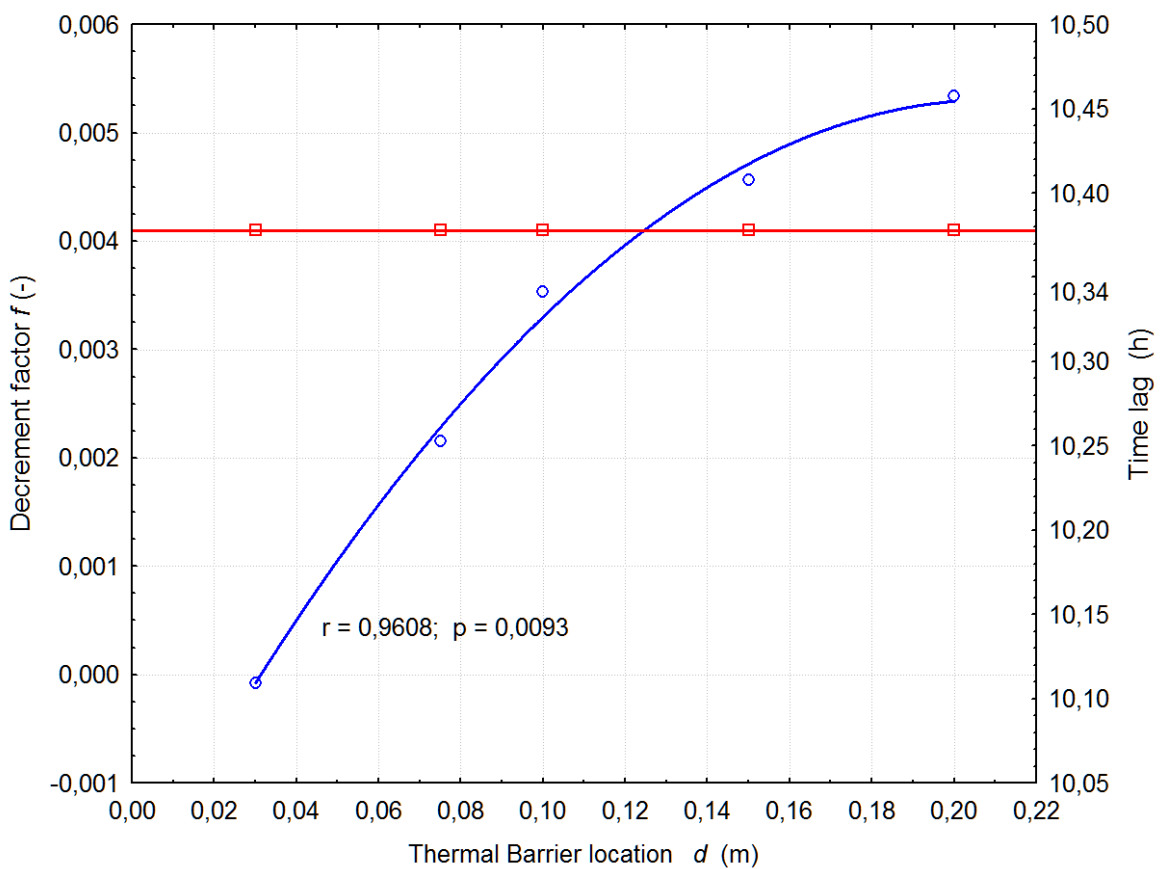
Fig.14: The effect of the Thermal Barrier location on the time lag (blue line) and decrement

factor (red line) of the external wall component

TB semi-

Insulat.

Concrete.

18,9 °C

TB

13,9 5 °C

Ambien

Indoor

-16,26 °C

TB effective

0,075 m

d = 0,169 m
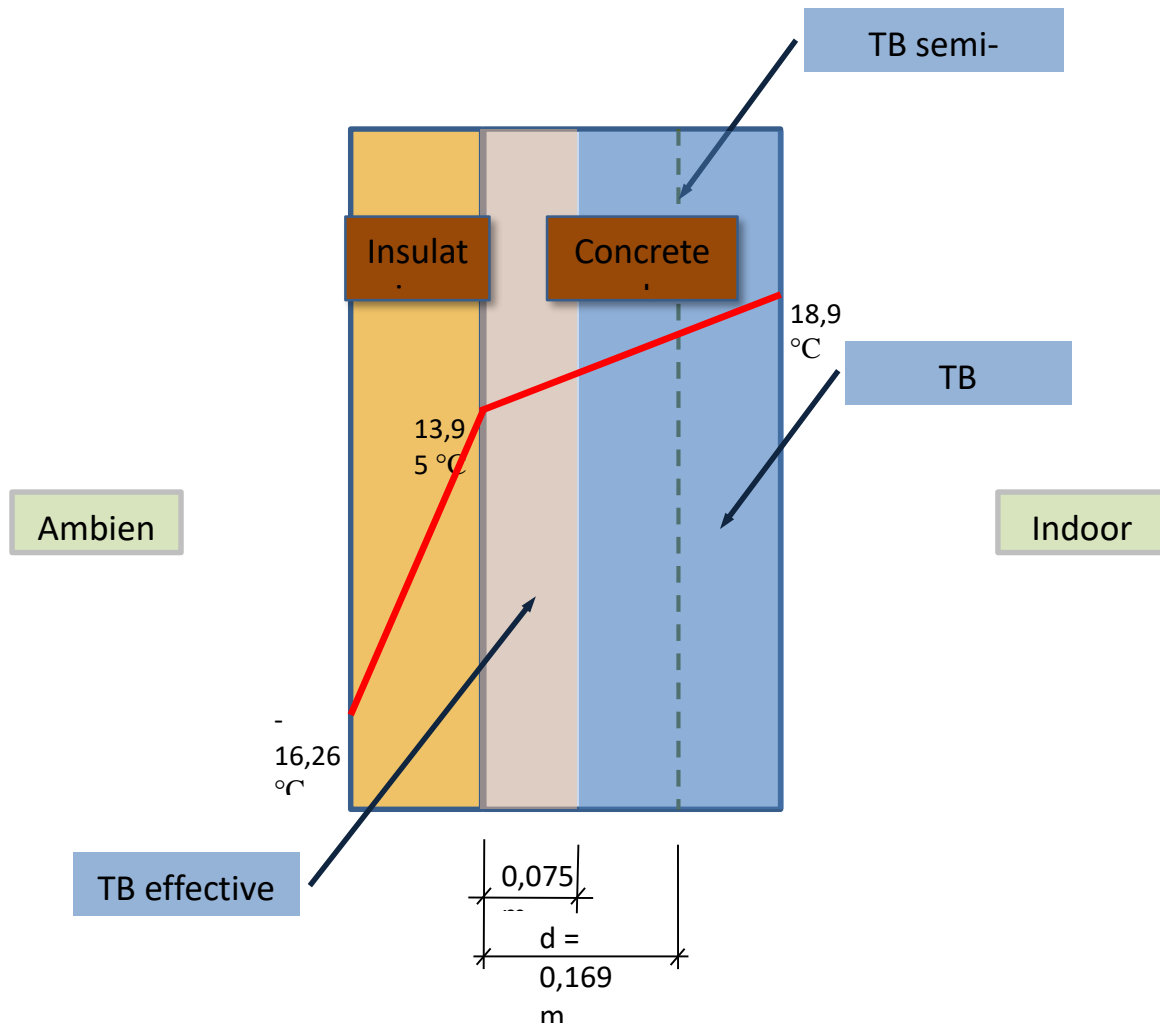
Fig.15: Temperature distribution in the two-layer external wall component under steady-state conditions equivalent to FMGS-PI controller's working mode I (Part II; no U-pipe system)
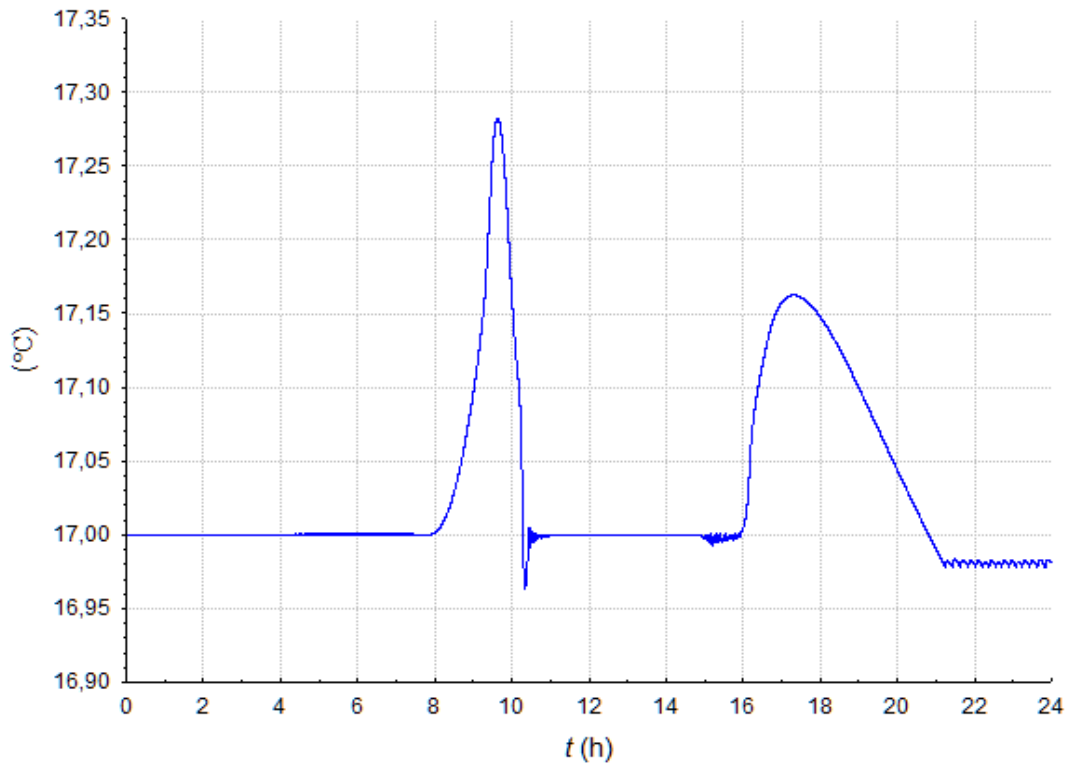
Fig.16: The TB semi-surface temperature variation for the TB location of *d*=30 mm and time period on 15th of February
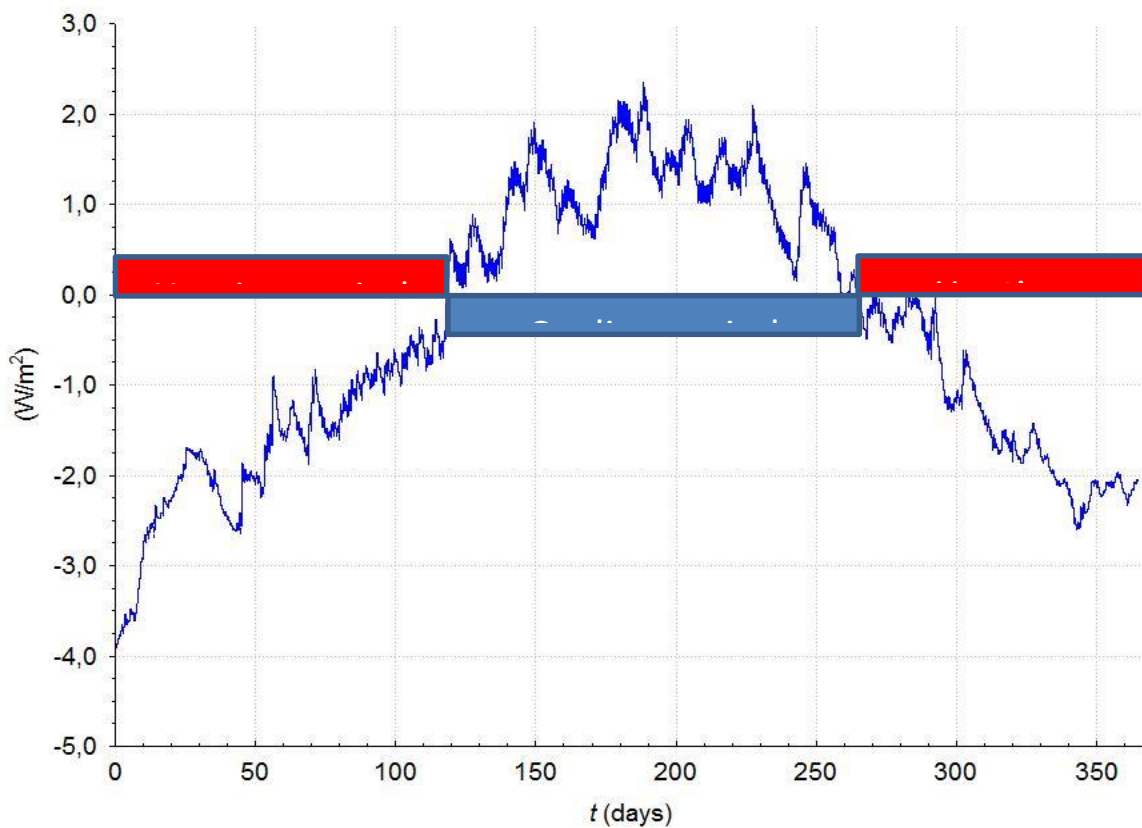
Fig.17: Time-variations of the heat flux on the internal surface of the external-wall prefabricated component without TB U-pipe system
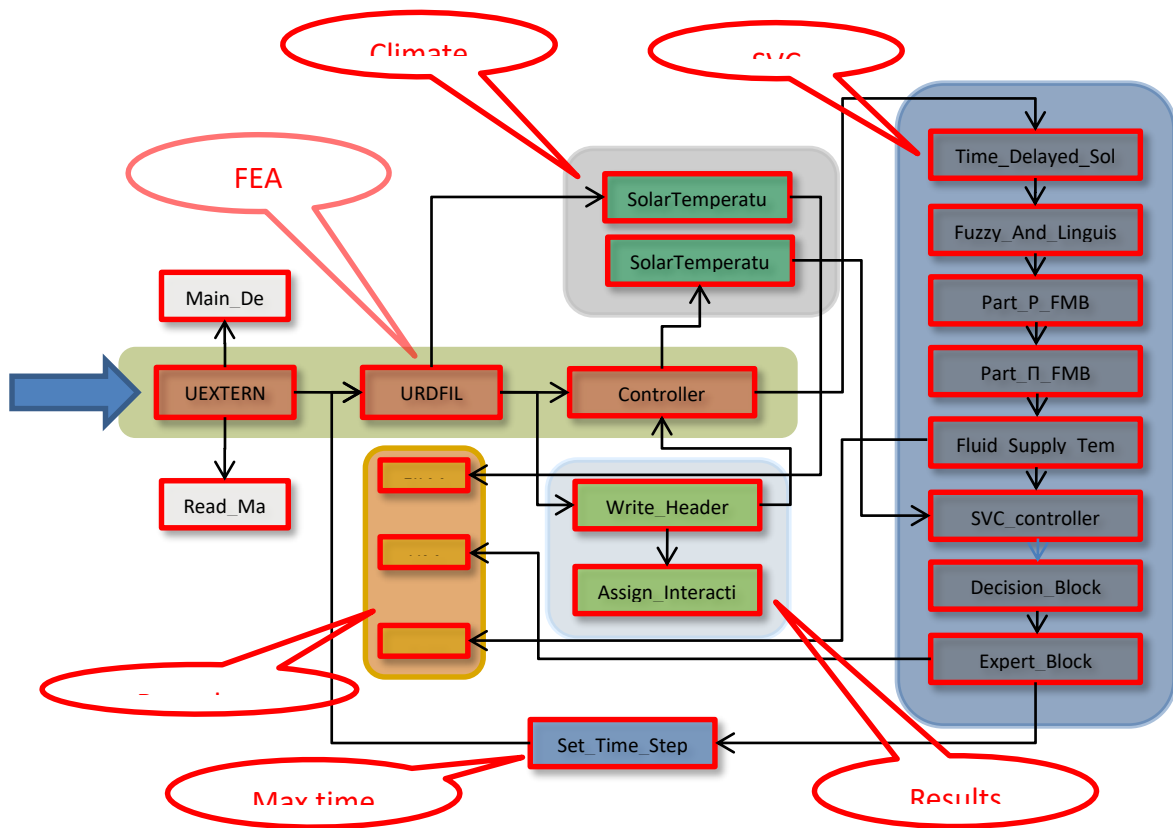
Fig.18: FORTRAN program controlling FE simulations of the TB annual performance and stability using ABAQUS [16]
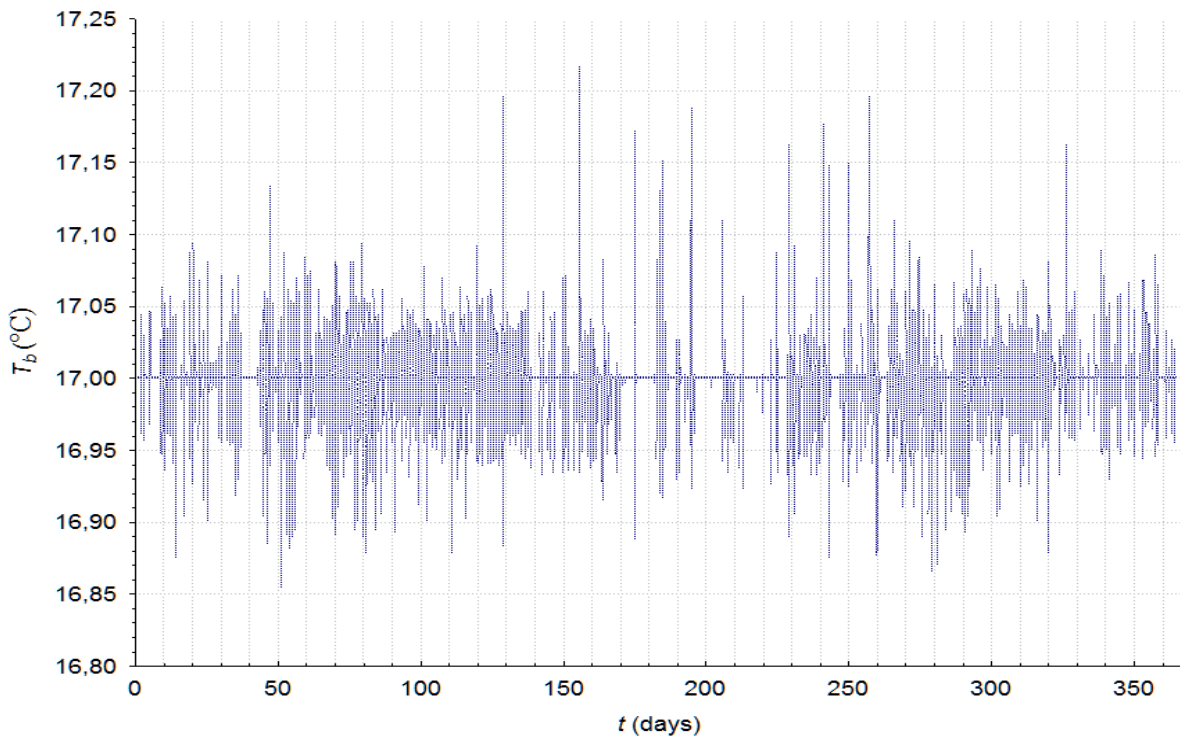

Fig.19: Control effect of SVC (case 'a') on the TB temperature stability during one year
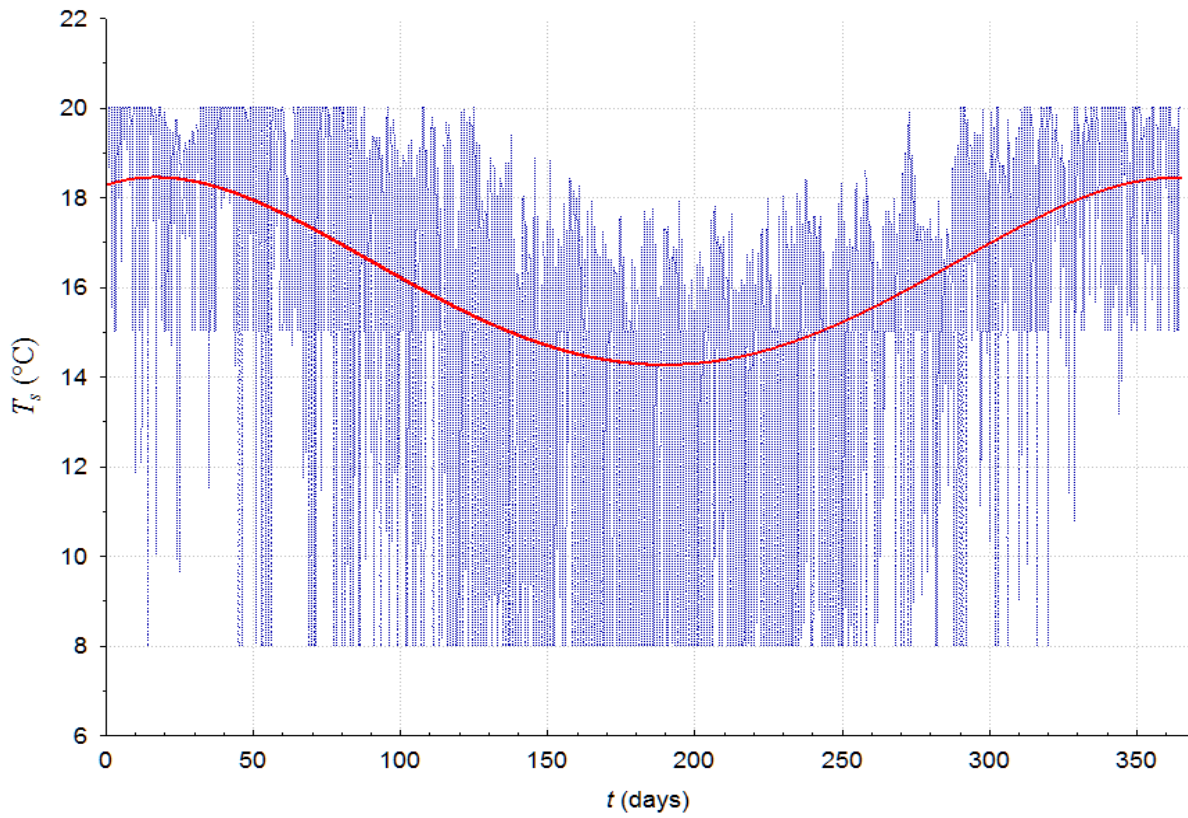
44

Fig.20: The annual variation of the TB fluid supply temperature
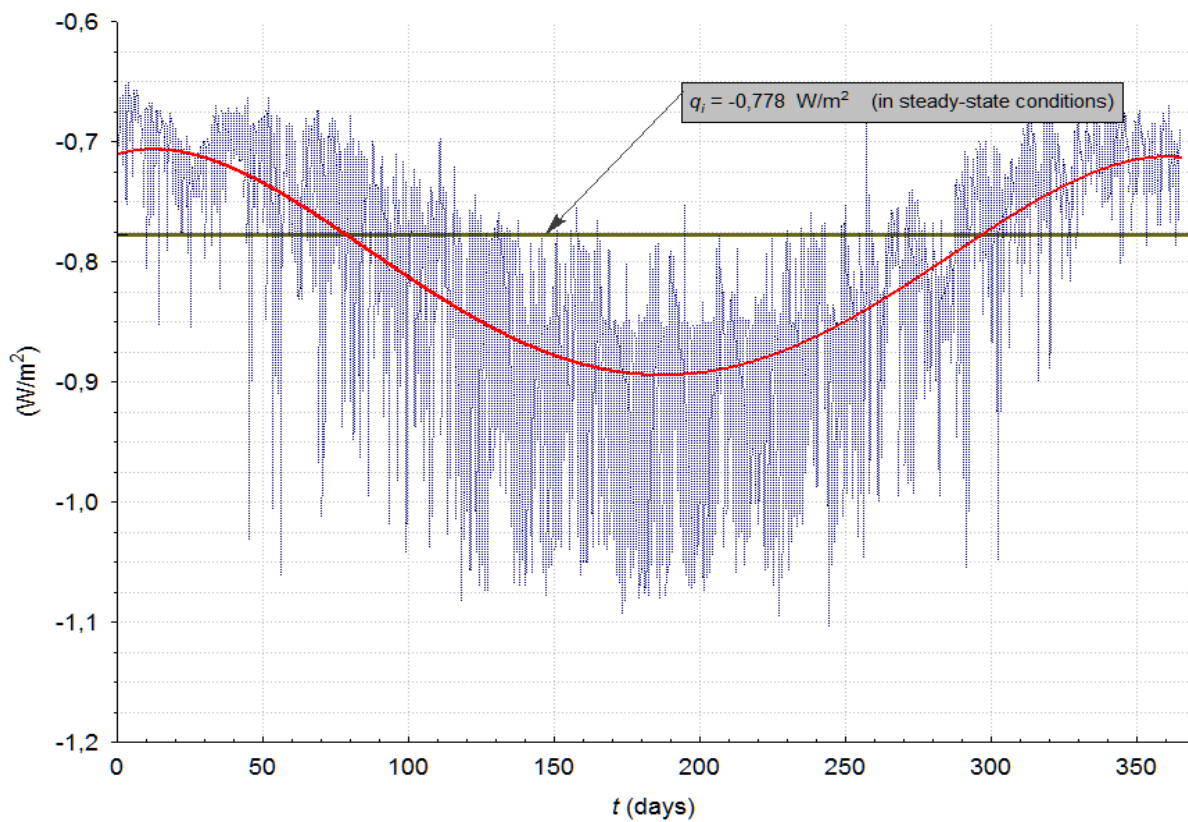

Fig.21: The annual variation of the heat flux on the internal surface of the external-wall
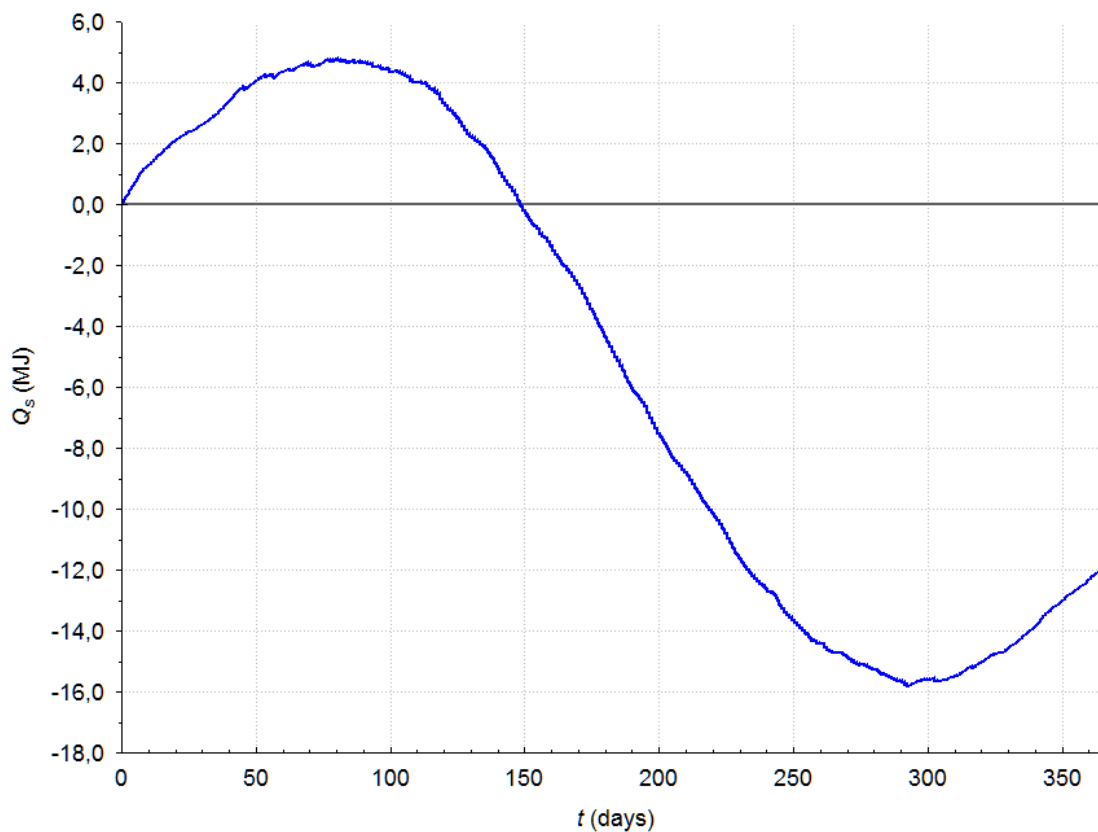prefabricated component

45

Fig.22: The cumulated diagram of the total amount of energy transferred from/to the fluid during one year time period
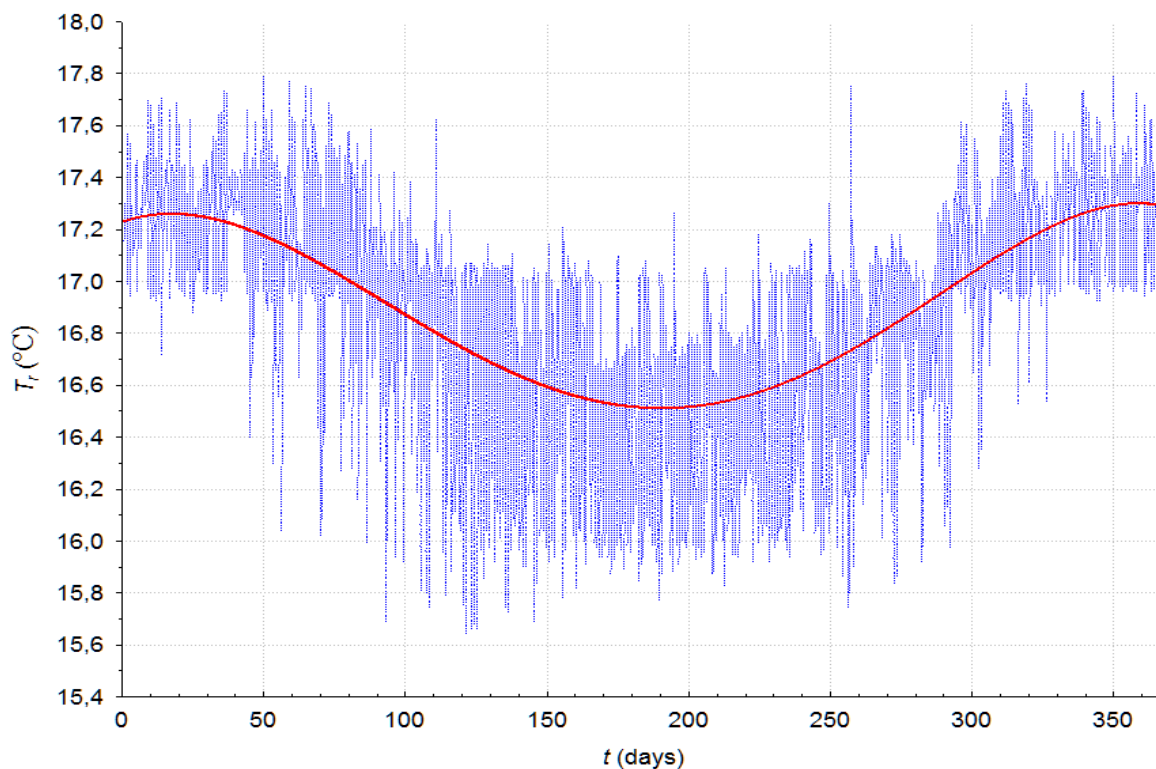

Fig. 23: The annual variation of the fluid return temperature of TB U-pipe system
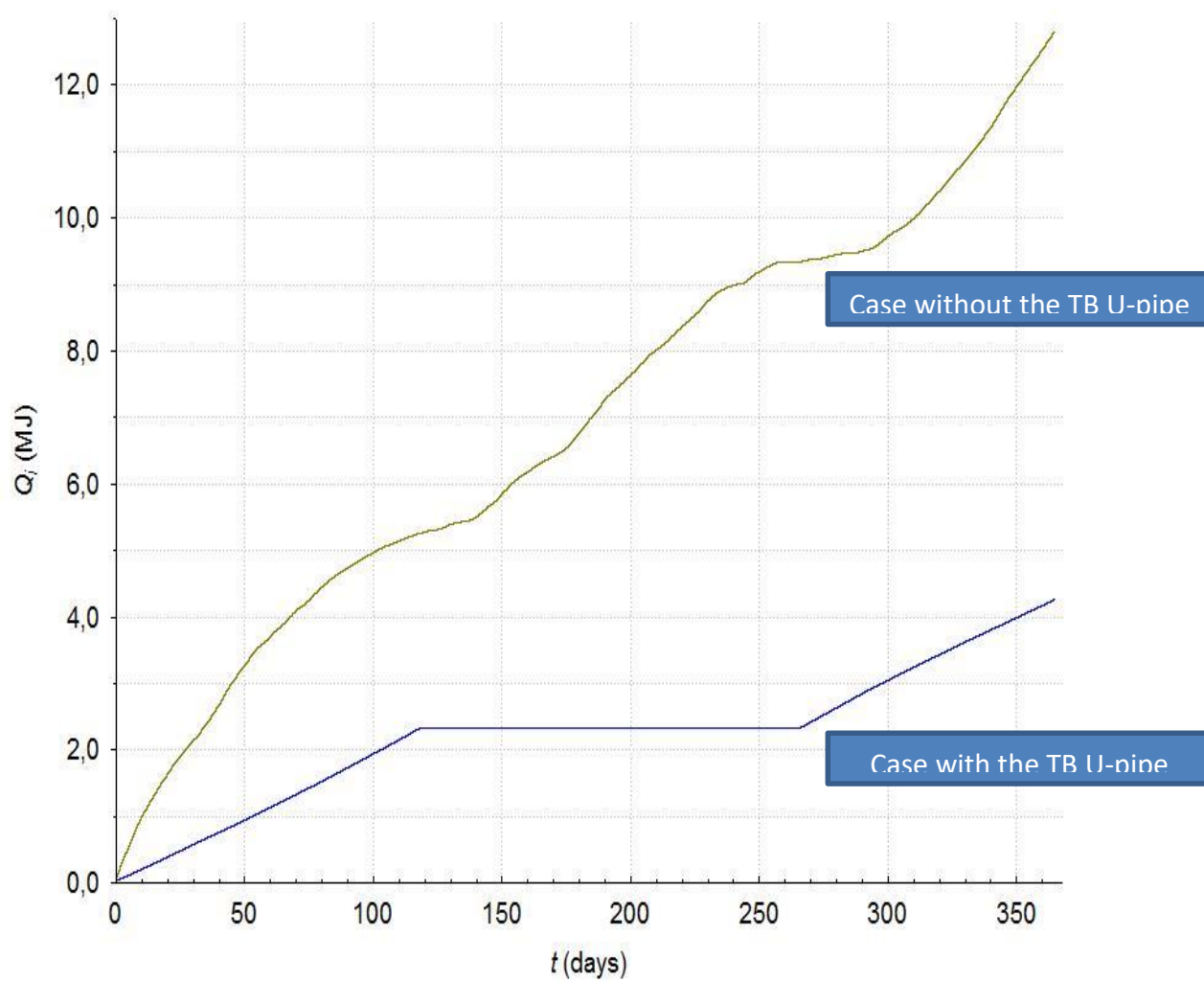
Fig.24: The heating and cooling demands expressed as a function of the cumulated value of
for the external-wall prefabricated component with and without TB U-pipe system

Tables

Tab.1: Material properties of layers of external-wall prefabricated component

	Layer thickness [m]	Heat conduction [W/m K]	Density [kg/m³]	Specific heat [J/kg K]	Thermal resistance [m²K/W]
Outer insulation (polystyrene)	0,125	0,035	40	1460	3,57
Lightweight concrete core structure	0,150	0,470	1200	840	0,32
Inner insulation (polystyrene)	0,125	0,035	40	1460	3,57
Total thermal resistance R_c:					7,46

Tab.2: Physical parameters of water and polypropylene

	Heat conduction [W/m K]	Density [kg/m³]	Specific heat [J/kg K]
Water	0,58	998	4187
Polypropylene	0,40	910	2450

Tab.3: Total annual heat demand for the reference residential house according to ISO standard [20]

Heat losses			
Type of thermal component/ventilation	U-value (W/m^{2}K)	Area of the component (m^2)	Heat losses through the component/ventilation (kWh/a)
External walls	0,131	285,4	3 283,2
Windows	0,8	41,99	2 922,3
Roof	0,15	137,7	1 796,9
Slab over the basement	0,15	137,7	1 280,1
Total heat losses through the envelope components			9 282,5
Heat demand for ventilation	Air exchange rate = 145,8 m^3/h	Recovery coefficient 0,7	519,0
Total heat losses			9 801,5
Heat gains			
Total solar heat gains			4 986,1
Total domestic heat gains			2 570,0
Heat demand			
Total heat demand			2 245,4